PATENT APPLICATION

IN THE UNITED STATES PATENT AND TRADEMARK OFFICE

In re application of

Yukako FUKUHIRA, et al.

Docket No: Q90825

Appln. No.: 10/552,685

Group Art Unit: 1615

Confirmation No.: 3807

Examiner: Caralynne E. Helm

Filed: October 11, 2005

For: BIODEGRADABLE FILM HAVING HONEYCOMB STRUCTURE

DECLARATION UNDER 37 C.F.R. § 1.132

Mail Stop Amendment
Commissioner for Patents
P.O. Box 1450
Alexandria, VA 22313-1450

Sir:

I, Yukako Fukuhira, hereby declare and state that:

I am a citizen of Japan.

I received a B.S. degree in March, 1999 from the Department of Applied Chemistry, Faculty of Science and Engineering, Chuo University, Japan, an M.S. degree in March, 2001 from the Department of Applied Chemistry, Graduate School of Science and Engineering, Chuo University, Japan, and a Ph.D. degree in March, 2009 from the Division of Chemistry, Graduate School of Science, Hokkaido University, Japan.

Since April 1, 2001, I have been employed by Teijin Limited, Tokyo, Japan, in Research Laboratories III, Integrative Technology Research Institute, New Business Development Group, and have been engaged as a researcher in polymer science and biomaterials.

I am an inventor of the invention described and claimed in the above-identified application, and I am familiar with the Office Action dated February 2, 2010 and the Advisory Action dated June 24, 2010.

In order to demonstrate the unpredictability of forming a honeycomb structure depending on the particular amphiphilic molecule used, the following experimentation was conducted by me or under my direct supervision. Also, the following comments are provided in connection with having a correct understanding of the description of Johnsson / Huang.

a) The hexagonal structure of DOPE (Dioleoylphosphatidylethanolamine) in water is different from that in the present invention

According to the Examiner's understanding, DOPE in water forms a stable hexagonal structure since it is a water-insoluble amphiphilic molecule. However, the actual structure is a cylindrical one with infinite length, though its cross-section is circular and similar to the hexagonal structure of the present invention. In this regard, I refer to Figure 3 on page 7 of the attached Reference Material 1 (PMC Biophysics article). Also, I refer to the attached PowerPoint Fig. 1, which is based on Figure 3 of Reference Material 1.

On the other hand, the honeycomb structure of the present invention is formed by fine spherical droplets of water as a template. Though it can be seen as hexagonal from the above, it has a spherical void internally. The honeycomb structure of the present invention is not an array of hexagonal cylinders, but rather it has interconnected spherical voids internally. A void in the film is connected to adjacent six voids to form interconnected voids, which is a completely different structure from that in Johnsson or Huang. In this regard, I refer to the attached PowerPoint Fig. 2.

As a consequence, an ordinary artisan knowing the difference of the structures would not have utilized the teachings of Johnsson or Huang, i.e., a cylindrical structure, to prepare the honeycomb structure of the present invention.

b) The size is greatly different

In addition of the difference in shape mentioned above, the size is greatly different as well. Whereas the diameter of the hexagonal cylinder in Figure 3 of Reference Material 1 showing DOPE in water is 7.34 nm (see PowerPoint Fig. 1; the diameter is calculated based on the values given in section 2.3 of Reference Material 1, i.e., 2 x 15.9 Å + 2 x 20.8 Å), the diameter in PowerPoint Fig. 2, i.e., the present invention, is about 5 μm. Namely, the difference is about 1000 times. This indicates that the formation of the hexagonal structure described in Johnsson / Huang is a completely different physical phenomenon from the formation of the honeycomb structure in the present invention.

c) DOPE does not form a hexagonal structure in organic solvents

It was common technical knowledge that the hexagonal structure in Johnsson / Huang can only be found in water, so it could not have expected for an ordinary artisan to prepare the hexagonal structure in organic solvent.

d) A honeycomb film could not be prepared by using cholesterol, an amphiphilic molecule

If the Examiner were correct in that any amphiphilic molecule can be used to form the honeycomb structure of the present invention or Maruyama et al., it is deduced that one can prepare a honeycomb structure by using cholesterol, an amphiphilic molecule. See page 559 of the attached Reference Material 2 ("Intermolecular and Surface Forces").

However, according to the experiment shown below, a honeycomb structure of the present invention cannot be prepared by using cholesterol as an amphiphilic molecule. This means the Examiner's inference that the honeycomb structure can be prepared by utilizing any amphiphilic molecule is incorrect.

[Experiment 1]

A chloroform solution of polylactic acid (molecular weight: 100,000) (5 g/L) was mixed with cholesterol as a surfactant in a ratio of 10:1. The mixture was cast on a glass plate and allowed to stand under a condition at room temperature and at a humidity of 70%. The solvent was gradually evaporated off for preparing a honeycomb structure. Namely, the preparation condition was completely identical to the examples of the present description except for the amphiphilic molecule used.

However, the resultant film did not have a honeycomb structure. The attached PowerPoint Fig. 3 is an optical photomicrogram of the film.

[Experiment 2]

A chloroform solution of polylactic acid (molecular weight: 100,000) (5 g/L) was mixed with cholesterol as a surfactant in a ratio of 200:1. The mixture was cast on a glass plate and allowed to stand under a condition at room temperature and at a humidity of 70%. The solvent was gradually evaporated off for preparing a honeycomb structure.

However, the resultant film did not have a honeycomb structure. The attached PowerPoint Fig. 4 is an optical photomicrogram of the film.

In view of the above, I conclude that the formation of a honeycomb structure is unpredictable and depends on the type of amphiphilic molecule used. Further, I conclude that a skilled artisan considering the cited art would not have been able to predict that DOPE in

Johnsson and Huang, which forms a cylindrical structure with infinite length in water, could be used to form a honeycomb structure as in the present invention.

I declare further that all statements made herein of my own knowledge are true and that all statements made on information and belief are believed to be true; and further that these statements were made with the knowledge that willful false statements and the like so made are punishable by fine or imprisonment, or both, under Section 1001 of Title 18 of the United States Code, and that such willful false statements may jeopardize the validity of the application or any patent issuing thereon.

Date: February 2, 2011 By: Yukako Fukuhira
Yukako Fukuhira

Reference Material 1

PMC Biophysics

PhysMathCentral

Open Access

Mini-review

The multiple faces of self-assembled lipidic systems

Guillaume Tresset

Address: Laboratoire de Physique des Solides, Université Paris-Sud, CNRS, UMR 8502, F-91405 Orsay Cedex, France

Email: Guillaume Tresset - tresset@lps.u-psud.fr

Published: 17 April 2009

PMC Biophysics 2009, 2:3 doi:10.1186/1757-5036-2-3

Received: 29 September 2008
Accepted: 17 April 2009

This article is available from: http://www.physmathcentral.com/1757-5036/2/3

Abstract

Lipids, the building blocks of cells, common to every living organisms, have the propensity to self-assemble into well-defined structures over short and long-range spatial scales. The driving forces have their roots mainly in the hydrophobic effect and electrostatic interactions. Membranes in lamellar phase are ubiquitous in cellular compartments and can phase-separate upon mixing lipids in different liquid-crystalline states. Hexagonal phases and especially cubic phases can be synthesized and observed in vivo as well. Membrane often closes up into a vesicle whose shape is determined by the interplay of curvature, area difference elasticity and line tension energies, and can adopt the form of a sphere, a tube, a prolate, a starfish and many more. Complexes made of lipids and polyelectrolytes or inorganic materials exhibit a rich diversity of structural morphologies due to additional interactions which become increasingly hard to track without the aid of suitable computer models. From the plasma membrane of archaebacteria to gene delivery, self-assembled lipidic systems have left their mark in cell biology and nanobiotechnology; however, the underlying physics is yet to be fully unraveled.

PACS Codes: 87.14.Cc, 82.70.Uv

1. Introduction

Lipids are the building blocks of cellular compartments. By self-assembling into bilayers, they form fluid membranes that act as relatively impermeable barriers to the passage of most water-soluble molecules. Lipid membranes enclose the cell machinery and protect it from the extracellular environment [1]. They likewise maintain the characteristic differences between the contents of each compartments and the cytosol. They accommodate a number of specialized molecules performing crucial functions to the life of the cell: ion channels pumping protons across the plasma membrane [2], nuclear pore complexes controlling access to and from the nucleus [3,4], or rotary motors synthesizing ATP [5,6]. Several of membrane proteins and glycosphingolipids

are used as receptors by viruses and pathogens, including the Alzheimer's associated amyloid peptide [7-9].

Lipids share with other amphiphilic molecules the ability to self-assemble in solution into more or less complex aggregates, provided their density exceeds a certain critical micellization concentration (cmc) which depends upon their chemical structure and the ions present [10,11]. A typical cmc value for bilayer-forming lipids ranges from 10^{-10} to 10^{-6} M while micelle-forming lipids require 10^{-5} up to 10^{-2} M in the bulk solution [12]. The traditional view of the aggregation of amphiphilic molecules is based on the poor solubility of hydrocarbons in water, leading to what is known as the hydrophobic effect [13]. The presence of hydrocarbon residues induces the formation of a cavity in the water structure which causes an increased degree of order and consequently a significant decrease in the entropy of water [14,15]. When hydrocarbon residues meet upon an effective long-range attractive force [16,17], the cavities fuse with one another and expel water from the interface releasing entropy to the solution. This leads to the spontaneous formation of stable aggregates [18].

The hydrophilic headgroup – although not driving the aggregation – is responsible for the formation of an interface with water, and contributes to determine, in principle, the size and the shape of the aggregates through the interactions between the molecules. Simple geometric packing considerations allow the prediction of the final aggregate conformation given some elementary structural information on the amphiphilic molecules [19]. For this purpose, a geometric factor can be conveniently used, the dimensionless packing parameter p, defined as $p \equiv v/a_0 l_c$ where v is the hydrocarbon volume, a_0 the optimal headgroup area, and l_c the critical chain length beyond which the hydrocarbon chain can no longer be considered as fluid [12]. This parameter determines whether the amphiphiles will form spherical micelles ($p < 1/3$), non-spherical micelles ($1/3 < p < 1/2$), vesicles or bilayers ($1/2 < p < 1$), or inverted structures ($p > 1$). This heuristic picture holds as long as only one amphiphilic component enters the system. Otherwise, the interactions between components – electrostatic interactions, van der Waals forces, or hydrogen bonding – may reorganize the system following a complex phase diagram. For example, the mixing, in the absence of added salt, of cationic and anionic surfactants with different packing parameters, yields a segregation of the amphiphiles and gives rise to unexpected aggregates such as nanodiscs, punctured planes, and facetted icosahedra, depending on stoichiometry [20-23].

Due to their natural occurrence in living organisms, lipids, and the assemblies they generate, are of special interest not only for the understanding of the many biological functions they are involved in, but also in regard of their applications as biocompatible carriers of drug and gene for pharmaceutical and biomedical purposes [24,25]. Another reason for this interest lies in a high potential in material science and nanobiotechnology, for example, by constructing intricate nanoscale networks of enzymatic reactors [26,27], or by arranging inorganic materials with the liquid-crystalline regularity of lipid complexes used as templates [28].

This article gives an overview of the various structures and arrangements based on lipids which have attracted the attention of biophysicists in the last few years. The functions of particular lipid structures within the cell are presented and the applications in therapeutic treatments or nanobiotechnology are mentioned whenever applicable. Emphasis is also given to the underlying physics that governs self-assembly processes and vesicle formation. The review begins with lamellar membranes along with a discussion on the phase separation occurring in raft microdomains. Afterwards, the varying forms of non-lamellar phases are described. The long-range (> 20 nm) organized structures come next, including liposomes, exotic vesicles and tubular objects. The last section encompasses complexed systems where lipids are associated with other entities, namely biological polyelectrolytes and inorganic materials. The review ends with a short section which highlights the benefits given by computer simulations in complementing experimental data to visualize and to understand the mesoscale structure of self-assembled lipidic systems.

2. Various aspects of lipid membranes

2.1 Lipid bilayer and lamellar phase

Bilayers are certainly the most common structure formed by lipids as they are present in every cellular organisms. They can take various shapes within the cell: fairly flat in the plasma membrane, spherical and tubular for the components involved in vesicular transport, or with an intricate geometry in the endoplasmic reticulum and Golgi apparatus. In this section, we focus on the short-range (over a few nanometers) organization of lipid bilayers.

Figure 1A depicts a planar lipid membrane assembled into bilayer. This kind of flat membrane typically occurs for lipids with a packing parameter close to 1, which means that an individual lipid molecule fits to a cylinder (Figure 1C). Some of the phospholipids – one of the most frequently encountered family of lipids in nature [1,29] – have a tendency to form bilayer membrane, as is the case for 1-palmitoyl-2-oleoyl-*sn*-glycero-3-phosphocholine (POPC) shown in Figure 1B. The elastic properties of planar membranes are often described by the mean curvature modulus κ and the spontaneous curvature c_0 [30,31]. The vast majority of bilayers in a biological context have an asymmetry – the interior and exterior of the cellular compartments – resulting in a finite spontaneous curvature. Yet recent studies by small-angle x-ray and neutron scattering showed that the inner and outer leaflets of vesicle bilayers can be indistinguishable, even for highly curved vesicles with diameters down to 62 nm [32]. The mean curvature modulus gives a measure of the membrane rigidity. Most biological membranes have $\kappa \approx 30 k_B T$, where k_B is the Boltzmann constant and T the temperature, which makes them essentially flat at the molecular scale. κ depends upon the temperature and the bilayer composition – especially because of the interactions between the hydrocarbon chains of lipids [33,34] -, and contributes to the amplitude of membrane fluctuations [35].

Pure lipid bilayers are fluid at high temperatures but undergo a phase transition when the temperature decreases below a critical value [36]. The phase transition temperature is -2 °C for POPC

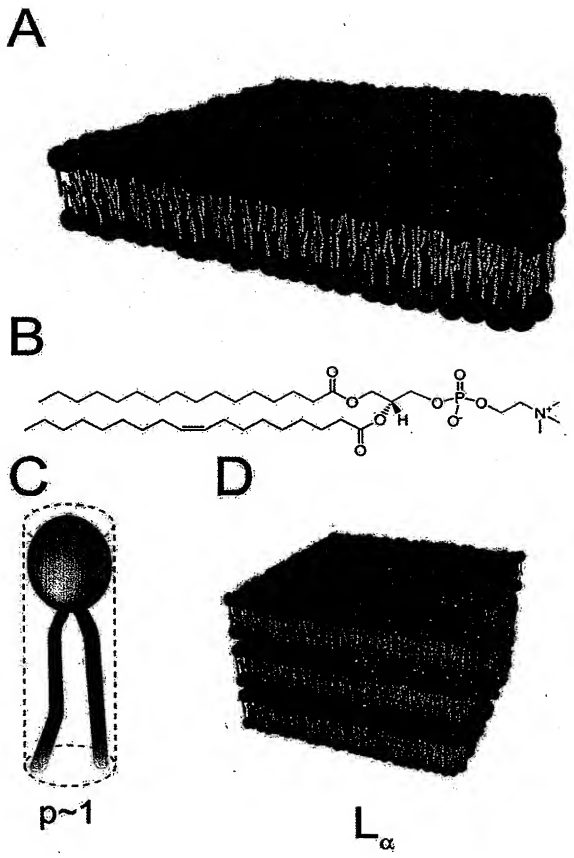

Figure 1
Lipid bilayer. (A) A flat membrane of lipids assembled into bilayer. (B) Chemical structure of 1-palmitoyl-2-oleoyl-*sn*-glycero-3-phosphocholine, a common phospholipid with $p \sim 1$ and which thereby forms flat bilayers. A schematic lipid molecule is depicted in (C), with the hydrophilic headgroup represented in red and the double hydrophobic alkyl chain in grey. The molecule fits to a cylinder making its packing parameter p close to 1. (D) Lamellar phase L_α of fluid lipid bilayers.

depicted in Figure 1B. According to its state, a lipid bilayer is said to be: in L_α liquid-crystalline phase when it is fluid with melted hydrocarbon chains; in L_β gel phase below the phase transition temperature; in L'_β tilted phase when the gel phase tilts relative to the layer normal; and in P'_β phase for tilted phase distorted by a periodic asymmetric ripple with a wavelength of the order of 100 Å [37,38]. The fluidity of lipid bilayer allows the membrane to reorganize spontaneously over a short time upon external stimulation: for instance, in response to an intense external electric field, biological membranes form submicrometer pores provided their transmembrane

potential exceeds a critical breakdown value [39,40]. With no longer electrical stimulation, the pores reseal over a period ranging from milliseconds to a few seconds depending on the membrane dynamics. This technique, known as electroporation [41], is used to inject plasmid DNA across the plasma membrane of cells.

Notice that several bilayers can pile up with a thin layer of water solution separating each of them; such a structure is referred to as lamellar phase, denoted L_α when the bilayers are fluid (Figure 1D). They are quite common with phosphatidylcholine (PC) lipids [36].

2.2 Phase separation and raft microdomains

A mixture of lipids in different phases – L_α and L_β, or liquid-disordered and liquid-ordered phases [42] for example – can phase-separate and give rise to the formation of raft microdomains in the bilayer. Each of the microdomains is enriched with lipids in the same liquid-crystalline phase. The size of microdomains ranges typically from a few nanometers to a few micrometers. Based on the properties of lipids in liposome membranes, domain models have long been proposed for native cell membranes [43,44]. The lateral segregation of lipids is believed to play a crucial role as it may govern a number of fundamental cellular processes such as signal transduction and inter and intracellular trafficking [45-48]. The self-organization into distinct domains permits the concentration of raft-associated specific receptors of proteins, which promotes the uptake of these proteins via the endocytic pathway. For example, a peptide sequence common to the Alzheimer's disease-associated Aβ peptide, the HIV-1 gp120 glycoprotein and the Prion protein was found to bind preferentially to raft-associated glycosphingolipids [7,49,50]. Such a peptide conjugated with a fluorophore constitutes a good raft marker for live cell imaging [51].

Biophysicists often investigate raft microdomains on supported lipid bilayers by atomic force microscopy (AFM), because this technique, unlike fluorescence microscopy, does not require the use of marker that may affect the phase separation of lipids [52-57]. Figure 2 shows a AFM image of a supported lipid bilayer on mica. The bilayer was made of a binary mixture of 1,2-dioleoyl-*sn*-glycero-3-phosphocholine (DOPC) in liquid-disordered phase and sphingomyelin in liquid-ordered phase. We can clearly see the domains of sphingomyelin emerging from the background of DOPC due to their larger size. A raft-associated protein is also visualized almost exclusively in the raft microdomains as expected [52].

Whether such idealized situations are transposable to live cells is still lively debated. Experiments on native lipid mixtures extracted from pulmonary membranes have shown the separation of two fluid phases [58], but the direct observation on live cell remains almost impossible due to the presence of anchored proteins and receptors that cover the membrane surface. Moreover, it seems that different experimental methods probe their own typical available length scales and therefore result in biased data. In an interesting computer study, Yethiraj and Weisshar [59] modeled a binary lipid mixture by using an Ising model on a square lattice comprising obstacles that

Figure 2
Three-dimensional atomic force microscopy image of raft microdomains. A binary mixture of 1,2-dioleoyl-*sn*-glycero-3-phosphocholine (black) and sphingomyelin (orange) forming a bilayer is immobilized on a mica substrate and exhibits a lipid phase separation. The height of the raft microdomains is ~7 Å. The yellow peaks correspond to a glycosylphosphatidylinositol-anchored protein which is located preferentially in the raft microdomains. The width of the scan is ~2 μm. Adapted from reference [52]. Used with permission.

mimic proteins anchored to the cytoskeleton. They reported that even at 5–10% by area of protein obstacles, the phase separation of lipids was dramatically reduced. This finding might bring the size of possible raft microdomains in live cell down to a few nanometers at best. However, another recent study reported that at physiological temperature, raft microdomains in the plasma membrane of an epidermoid carcinoma cell line coalesce upon the binding of cholera toxin B subunit to raft-associated ganglioside GM1, leading to the formation of raft clusters of a few micrometers in size [60].

2.3 Non-lamellar membrane structures

Lipids with packing parameter $p \sim 1$ form preferentially bilayers, or more generally, a lamellar phase made of bilayer sheets. For other classes of lipids and mixtures of lipids, the three-dimensional polymorphism can be quite diverse, accompanied by a complex phase diagram depending on temperature, pressure, molecular structure and concentration of components [61]. The pioneering work in this field was carried out by Luzzati and coworkers who studied lipid-water systems by x-ray scattering techniques and found a number of non-lamellar liquid-crystalline arrangements which can be categorized into hexagonal and cubic phases [62-64].

Hexagonal phases are made of thin lipid cylinders with a radius of a few nanometers and arranged on a two-dimensional hexagonal lattice (Figure 3). When the polar headgroup of lipids

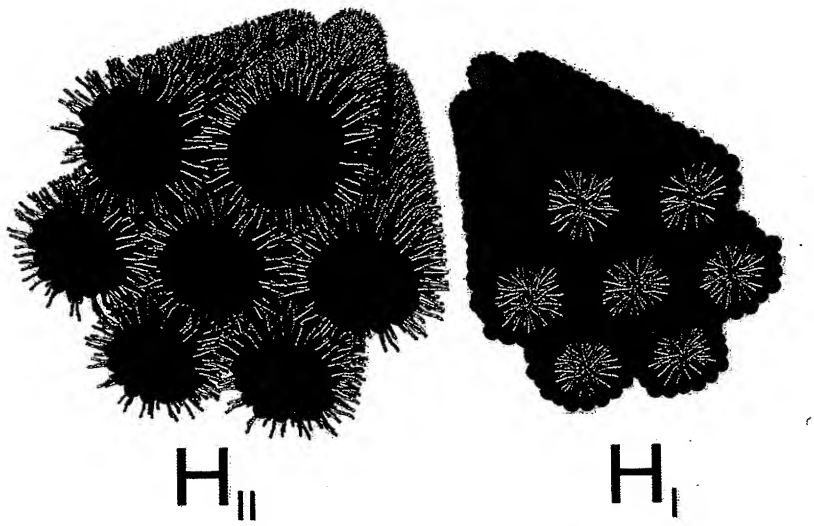

Figure 3
Illustration of hexagonal lipid phases. Inverted hexagonal (H_{II}) and micellar hexagonal (H_I) phases. The lipids are represented with the same conventions as on Figure 1, the hydrophilic headgroup in red and the hydrocarbon chains in grey.

is oriented towards the internal space of the cylinder, which is filled with water, the structure is called inverted hexagonal phase or H_{II} [65]. In contrast, when the internal volume is filled with the hydrocarbon chains, the phase is said to be micellar hexagonal H_I. Phosphatidylethanolamine (PE) is a class of lipids abundantly found in biological membranes and prone to form an inverted hexagonal phase [66]. At 20°C the radius of the water core in the cylinder is 15.9 Å for 1,2-dioleoyl-*sn*-glycero-3-phosphoethanolamine (DOPE) whose molecular length is 20.8 Å as inferred from x-ray diffraction reconstruction [67]. Below 20°C, DOPE can form a fluid lamellar L_α phase in coexistence or not with an inverted hexagonal H_{II} phase as the water content varies above ~10% (w/w) [68,69]. The propensity of PE lipids to form an inverted phase may be of high importance in relation to membrane fusion events. PE lipids may help their host membrane achieve highly curved intermediate structures during fusion, which is energetically favorable for the process [70,71].

The other category of non-lamellar structures is made of three-dimensional cubic phases which are subdivided into bicontinuous and micellar classes [72,73]. The inverse bicontinuous cubic phases consist of a single continuous curved lipid bilayer folded into a three-dimensional cubic network and separating two disjointed water compartments. Following the mathematical argument of periodic minimal surfaces [73,74], the inverse bicontinuous phases can exhibit three distinct morphologies [75,76] labelled *Ia3d*, *Pn3m* and *Im3m* (Figure 4), the latter being not well established experimentally. The additional sponge phase (L_3) can be viewed as a melted cubic phase because it shares the properties of bicontinuous cubic phases but does not have a long-

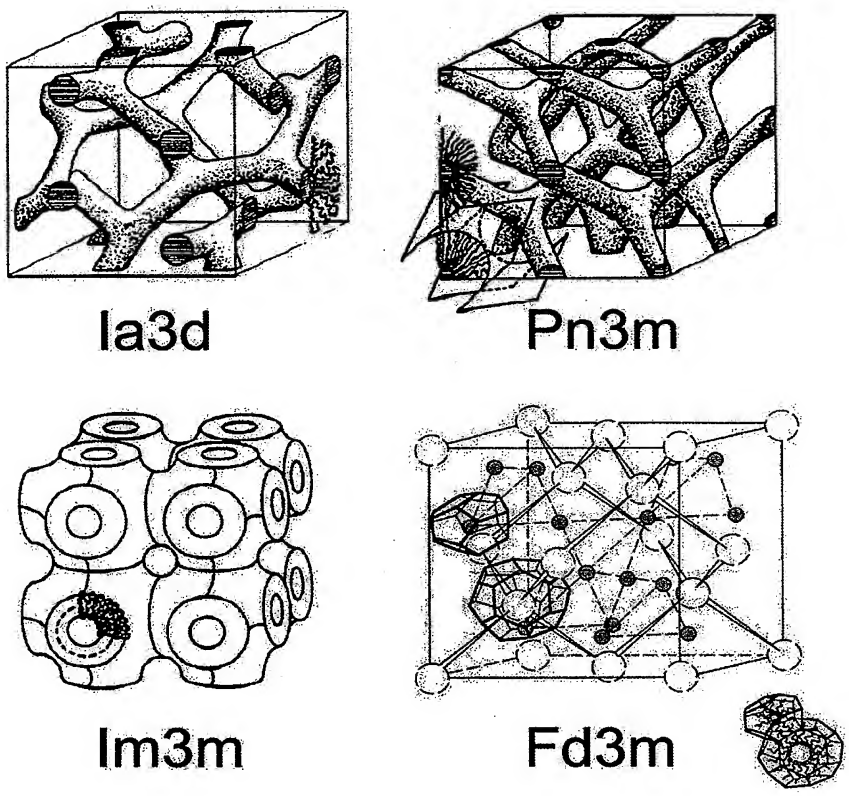

Figure 4
Schematic structures of lipid cubic phases. *Ia3d*, *Pn3m* and *Im3m* are the inverse bicontinuous cubic phases reported so far experimentally. *Fd3m* is an inverse micellar cubic phase found with mixtures of DOPC and glycerol. The two types of inverse micelle (open and grey spheres) with their polyhedral shapes are indicated on each site of the cubic lattice. Adapted from reference [73]. Reproduced by permission of the PCCP Owner Societies.

range order [77]. In the micellar cubic phase, the structure is made up of disjointed inverted micelles packed on a cubic lattice. The micelles are actually distributed in two populations of different sizes to allow a more efficient packing of space. This is the case for phosphatidylcholine-glycerol mixtures which form a *Fd3m* micellar cubic phase [78]. Figure 5 provides a close-up view on the internal structure of lipid nanoparticles exhibiting bicontinuous cubic, sponge, and inverted hexagonal phases.

There are many evidences that lipid membranes in cubic phase are ubiquitous in the biological world. They have been observed in the plasma membrane of archaebacteria [79], as well as in the endoplasmic reticulum and mitochondria of mammalian cells [80]. In structural biology, lipid cubic phases can be employed as matrices to crystallize membrane proteins enabling diffraction and thereby reconstruction with a high resolution [81-83].

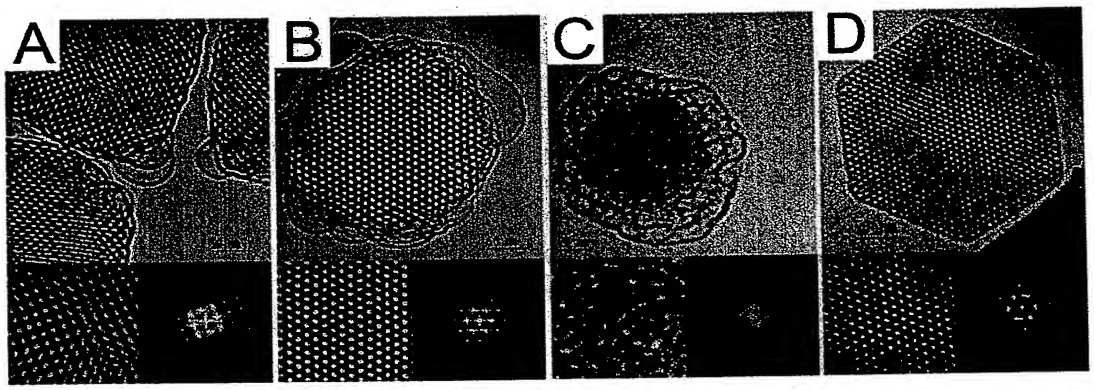

Figure 5
Cryo-Transmission Electron Microscopy micrographs of non-lamellar lipid nanoparticles. Inverse bicontinuous cubic phase nanoparticles viewed along the [001] (A) and [111] (B) directions. The Fourier transforms of magnified areas shown in the right-lower inserts of each micrographs are consistent with a body centered cubic phase *Im3m*. The nanoparticles are made up of a dispersion of glycerol monooleate (GMO), surfactants and polymeric stabilizers. (C) Sponge phase L_3 nanoparticles containing diglycerol monooleate (DGMO) and glycerol dioleate (GDO). (D) Inverted hexagonal H_{II} nanoparticles also based on DGMO and GDO but with a different fraction of stabilizer. Adapted from reference [75] with permission. Copyright 2005 by the American Chemical Society.

3. Vesicular and tubular shapes

3.1 Liposomes

When lipids are dispersed in an excess of aqueous solvent, they are no longer able to form a continuous phase and make instead a suspension of aggregates exhibiting locally one of the phases described earlier. For a lipid component with a packing parameter between 1/2 and 1, the resulting aggregates are spherical vesicles comprising one or several bilayers, and are called liposomes [25,84,85]. Liposomes come in varying size and lamellarity (Figure 6) [86]: the nomenclature usually distinguishes the small unilamellar vesicles (SUV, 10~100 nm), the large unilamellar vesicles (LUV, 100~1000 nm), the multilamellar vesicles (MLV, with an onion-like layered membrane), the oligovesicular vesicles (OVV, small vesicles incorporated into a bigger one), and the giant unilamellar vesicles (GUV, > 1 μm), but other morphologies frequently occur as well. Liposomes can be prepared by spontaneous swelling of a lipidic film hydrated with an excess of the desired aqueous solution [87]. After formation, they are in general not colloidally stable and slowly aggregate and fuse into larger and more lamellar structures.

Submicrometer liposomes can be obtained with a narrow size distribution. Given that their membrane is biocompatible and impermeable to hydrophilic molecules, they can be conveniently used as nanocapsules. Consequently, submicrometer liposomes have attracted a strong interest in the biomedical and pharmaceutical sectors for their applications in drug delivery [24,88-90]. Liposomes are not just merely passive capsules transferring drugs into cells, their membrane can be engineered, for example so as to release the cargo inside a low pH environment such as in the endosome [91]. Many kinds of site-specific ligands such as antibodies, receptors

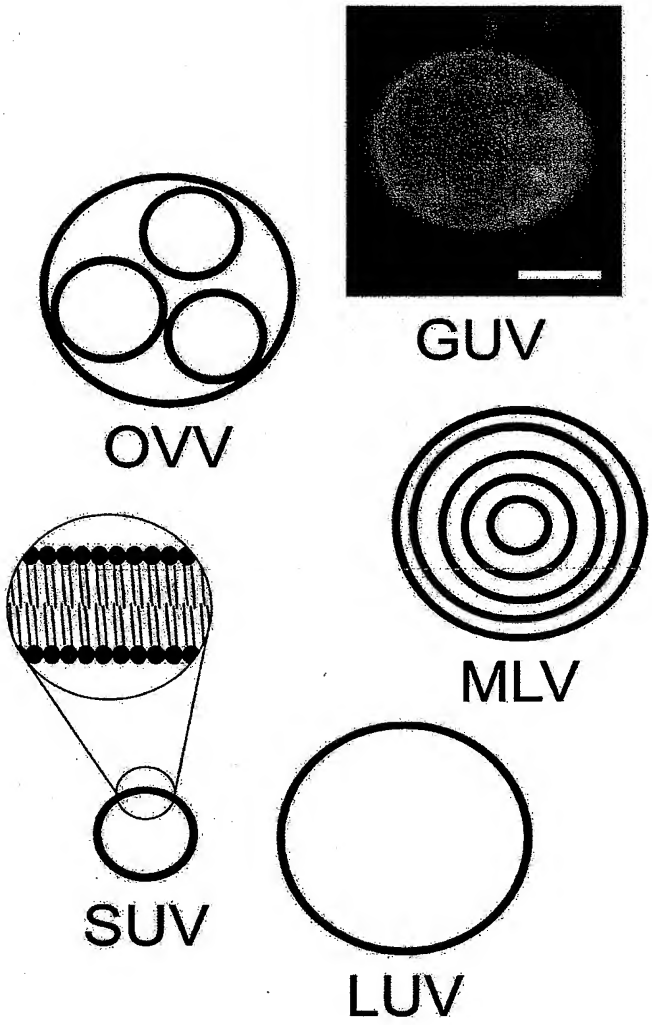

Figure 6
Liposome morphologies. Liposomes are presented with respect to the shape, size and number of bilayers. SUV = small unilamellar vesicle, LUV = large unilamellar vesicle, MLV = multilamellar vesicle, GUV = giant unilamellar vesicle, OVV = oligovesicular vesicle. The short-range structure of the lipid bilayers is shown in the magnified view. The GUV on the fluorescence picture is made of a mixture of phospholipids and fluorescent dye, and contains three red-fluorescent 200-nm polystyrene spheres which can move freely within the vesicle. The scale bar is 5 μm. Adapted from reference [99] with permission. Copyright 2005 by the American Chemical Society.

and peptides can be anchored to the membrane, directing the cargo to designated cell types [92]. The grafting of poly(ethylene glycol) (PEG) at the surface of a liposome carrier enables an extended circulation lifetime in the body [93]. Other applications include the use of liposomes as marker for ultra sensitive detection of biological toxins [94,95], or in binding assays of peptides to membrane receptors [51,96].

Giant vesicles occupy a privileged place in biophysics because their micrometer size allows a direct observation under optical microscope. They can be conveniently used as model of cell membrane for investigating biological processes in controlled environment, as well as for bioanalytical purposes [27,97]. The electrically-induced fusion of giant vesicles gives insights into the response of biological membranes to electric fields; it reveals for instance the existence of a threshold intensity related to the critical transmembrane potential [39,98-101]. The activity of particular ion channels embedded into giant liposomes can be recorded via patch-clamp methods [102]. Giant vesicles also constitute a good biomimetic environment for monitoring enzymatic reactions [103,104], and more fundamentally, they can be envisioned as a minimal system for constructing an artificial cell assembly expressing genes [105-107].

3.2 Exotic vesicles

The shape of lipid vesicles at equilibrium is not limited to a sphere. A large variety of shape deformations on giant vesicles are achievable by changing the external constraints on the membrane, namely the osmotic pressure difference between the interior and exterior of the vesicle [108] and the temperature [109]. The equilibrium shape of the vesicle can be fully determined by the area difference elasticity (ADE) model [110,111], which implies an additional term to the curvature energy of the membrane. This energetic term arises from the deviation in the total area difference between the inner and outer leaflets. Minimizing the thus-obtained free energy leads to the final shape. Complex two-dimensional phase diagrams can be numerically calculated, and the morphology of vesicles is then obtained as a function of a dimensionless measure of the volume-to-area ratio and of the intrinsic area difference which indicates the preferred curvature of vesicles [111].

Such calculations predict for phospholipid vesicles, a structural hierarchy of unexpected shapes such as rackets, boomerangs, and starfishes [112,113], and point out the existence of a critical point in the phase diagram where minute variations of membrane parameters can induce large shape transformations. Other shapes include stomatocytes, discocytes, prolates, and pears (Figures 7A, B and 7C) and have been reported experimentally with ternary mixtures of fluid lipids by adding salt into the extravesicular solution so as to apply an osmotic pressure difference [114].

In the case where the membrane of vesicles experiences a phase separation into raft microdomains, a term arising from the line tension at the phase boundary must be added to the free energy [115]. It results in complicated morphologies where the domains impose locally their preferred curvature and generate budding portions on the surface of vesicles [116-118]. Two photon fluorescence microscopy on giant vesicles provides a direct way to visualize lipid domains labeled with distinct fluorescent dyes. It gives information about the deformations induced on the vesicles (Figure 7D) [119-122] and allows to evaluate quantitatively the dynamics of raft microdomains [114,123,124].

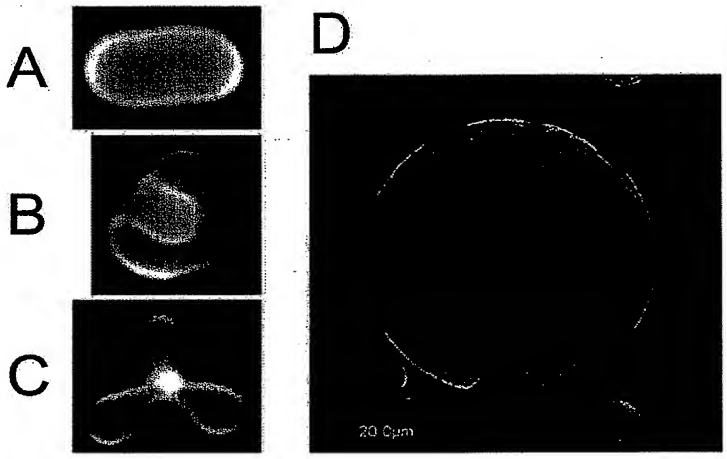

Figure 7
Exotic vesicles. (A) Prolate, (B) stomatocyte, and (C) starfish vesicles made of a ternary mixture of saturated and unsaturated phospholipids and cholesterol, in presence of ~1 mM of sorbitol at 60°C. Reprinted figure with permission from reference [114]. Copyright 2008 by the American Physical Society. DOI: 10.1103/PhysRevLett.100.148102 (D) Three-dimensional confocal microscopy image of a giant vesicle labeled with two distinct fluorescent dyes staining the liquid-ordered and liquid-disordered phases of a ternary mixture of lipids. Reproduced from reference [123] by permission of the PCCP Owner Societies.

3.3 Lipid nanotubes

Electron microscopy has revealed the existence of tubulo-vesicular elements interposed between the endoplasmic reticulum and the Golgi apparatus in pancreatic rat cells [125]. It was suggested that these lipid nanotubes, abundant around the Golgi complex, interconnect adjacent Golgi elements and are involved in the transport of membrane outward along microtubules [126]. The directed transport of small membrane blebs along a lipid nanotube has been observed in red blood cells as well [127], supporting the idea of the general interconnection of cellular compartments by lipid nanotubes.

Lipid nanotubes consist of multiple lipid bilayers rolled up in a long cylinder [128,129]. Their inner diameter ranges from ~10 nm with synthetic lipids to hundreds of nanometers for natural phospholipids, and their length can reach up to several centimeters [130].

Because most phospholipids do not self-assemble into tubular shapes upon simple dispersion, phospholipid nanotubes must be obtained for example by pulling on the membrane of immobilized giant vesicles with a micropipette [131,132]. In doing so, complex tubulo-vesicular networks in which the transport of specific molecules between compartments is assured by controlled diffusion can be constructed in view of bioanalytical applications [27,132,133]. In other protocols, the lipid tube growth is induced by a fluid flow guided in microfluidic channels [130,134], or by the binding of steptavidin to biotinylated membranes [135].

It is worth noting that synthetic polymerizable phospholipids have enabled the spontaneous assembly of nanotubes with diameters of approximately 500 nm upon cooling down below the gel-to-liquid crystalline phase transition temperature [136,137]. Besides, elongated assemblies called cochleates have been derived from dioleoylphosphatidylserine (DOPS), simply by adding calcium chloride to a dispersion of liposomes. Cochleates are made of spiral multilayered structures (Figure 8) held together by a cation bridge, and have been used in drug delivery [138].

Following the spirit of research conducted on carbon nanotubes, studies on lipid nanotubes with attoliter void volume have been carried out. The typical nanotube diameter must lie in the range of ~10 nm, a curvature inaccessible to most of the lipid bilayers. Synthetic glycolipids presenting a single hydrocarbon chain are able to self-assemble into nanotubes of interdigitated lamellar layers stabilized thanks to a π-π stacking mechanism. Their inner diameter is about 10~15 nm, and their wall thickness up to ~15 nm [139] conferring a tubular persistence length of about 5 cm, that is, fifty fold as high as that of microtubules [140]. Interestingly, these glycolipids yield nanotubes with varying morphologies according to the degree of unsaturation of their hydrocarbon chain: twisted ribbon, coiled ribbon or nanotube without helical marking (Figure 9). The water confined within these nanotubes was shown to be highly structured with respect to the bulk [141].

4. Lipid-based complexes

Lipids can be complexed with virtually any materials provided that the electrostatic interactions are favorable. It is therefore impossible to review all the existing structures in a comprehensive manner. We will limit ourselves to the systems that have been extensively studied or that present a particular interest to biophysicists.

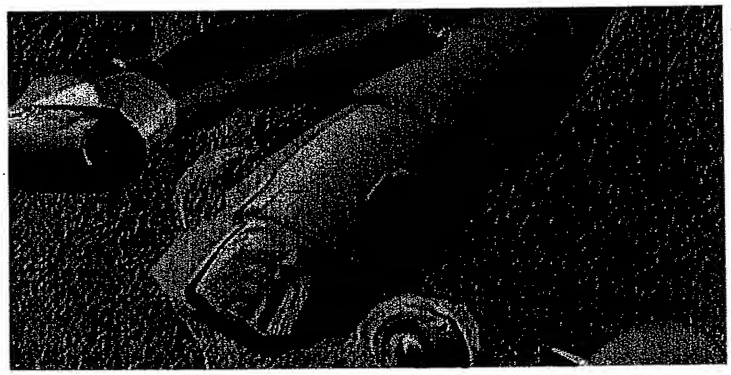

Figure 8
Transmission electron micrograph of cochleates. Transmission electron micrograph after freeze-fracture of cochleate cylinders prepared from anionic phosphatidylserine (PS) and calcium ions. The layered structure is clearly visible. The scale bar is 200 nm. Reproduced from reference [138] with permission. Copyright 2002 by Elsevier Science.

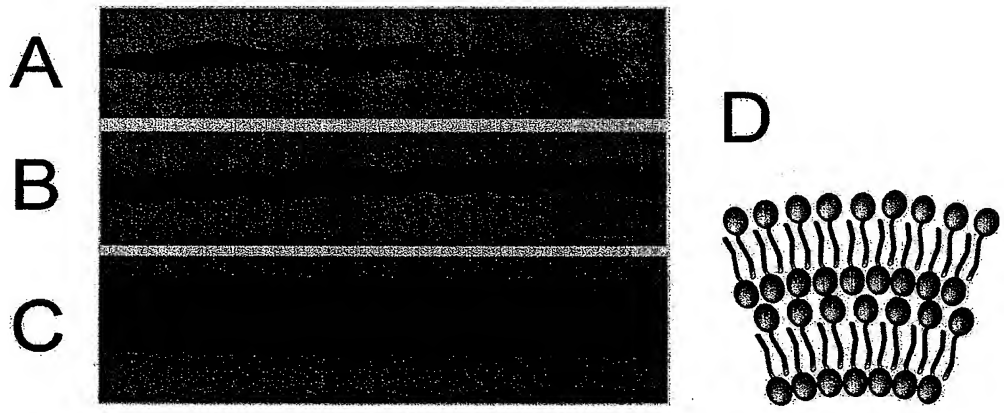

Figure 9
Morphologies of glycolipid nanotubes. Transmission electron microscope images of (A) twisted, (B) coiled, and (C) tubular one-dimensional assemblies of glycolipids. Reproduced from reference [128] with permission. Copyright 2005 by the American Chemical Society. (D) Schematic cross-section of the interdigitated lamellar layers of single hydrocarbon chain glycolipids in the nanotube membrane. The glycolipid headgroup is represented in red and the hydrocarbon chain in grey.

4.1 Lipid-DNA complexes or lipoplexes

Mesoscale assemblies made of lipids and DNA are perhaps the most documented self-assembled lipid-based complexes because they are a good case study of the intermolecular interactions between lipids and polyelectrolytes, and most importantly because they hold great promises for the future of gene therapy and protein delivery into cells [142-147]. Lipid-DNA complexes, also called lipoplexes, were first introduced some 20 years ago by mixing cationic liposomes with DNA, and allowed the effective transfer and expression of genes in cultured cells [148]. The encapsulation of DNA was by far more efficient than previous techniques involving liposomes because the cationic charge of the synthetic lipids enabled a 100-%-efficiency association with the negatively-charged DNA.

Several of the liquid-crystalline structures listed previously are recovered by lipoplexes (Figure 10). The complexed lamellar phase L_α^C consists of alternating monolayers of parallel DNA rods and lipid bilayers [149-151]. The spacing between the two-dimensionally condensed DNA rods is extremely regular and varies from nearly close packing (~24 Å) to about 60 Å depending on the lipidic charge density [152] and on the ions that screen the electrostatic repulsion created by the rods [153]. Moreover, there is a transbilayer correlation in the DNA ordering possibly controlled by the membrane rigidity which varies with the temperature [154]. Another structure often encountered is the complexed inverted hexagonal phase H_{II}^C where DNA rods are coated by a lipid monolayer and arranged on a two-dimensional hexagonal lattice. In comparison with the lamellar phase L_α^C, this structure is obtained either by increasing the spontaneous curvature

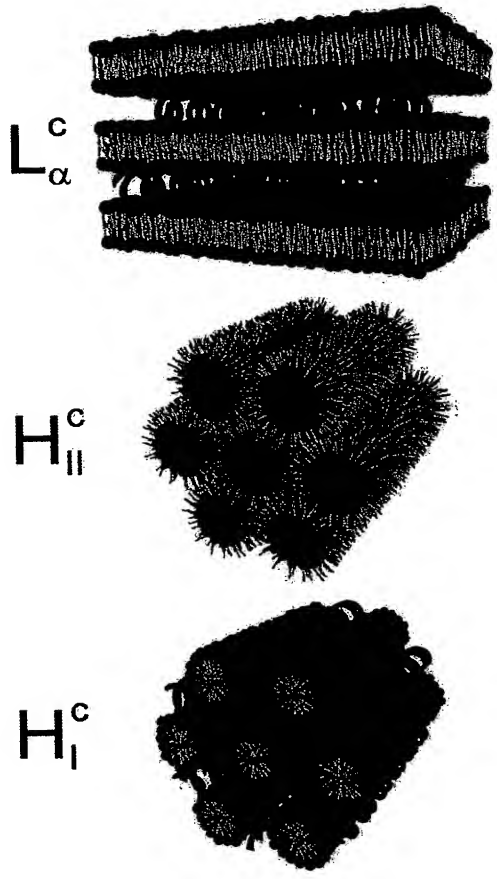

Figure 10

Lipoplex phases. Schematic representations of the phases of lipid-DNA complexes: complexed lamellar L_α^C, complexed inverted hexagonal H_{II}^C, and complexed micellar hexagonal H_I^C. The lipids are depicted in red (headgroup) and grey (hydrocarbon chain), while the DNA rods are in blue.

of the membrane or by lowering its mean curvature modulus down to a few $k_B T$ [155]. A complexed micellar hexagonal phase H_I^C was reported as well, where the DNA rods are arranged on a honeycomb lattice in the interstices of the lipid micelle arrangement [156].

Cationic lipids scarcely occur in cell membrane, they are only found in tiny amounts in neuronal tissues as cationic glycosphingolipids for instance [157]. As a result, the injection of synthetic cationic lipids into cells induces a number of toxic effects, often lethal, the more so as the lipid-to-DNA charge ratio of lipoplexes increases [158]. To address this issue, non-cationic phospholipids have been used in association with multivalent cations. By binding to the lipid headgroup, multivalent cations are able to turn the overall headgroup charge positive [159], making

the complexation with negatively-charged DNA electrostatically favorable. In doing so, the usual complexed liquid-crystalline structures are recovered, namely lamellar [160-162] and inverted hexagonal [163,164], the cations being intercalated so as to bridge the phospholipid headgroups and the DNA rods. Such systems have been proven as efficient as cationic lipids to transfer genes in cultured cells depending on the concentration and the valence of cations [164]. Monte Carlo calculations have shown that phospholipid-DNA complexes are the more stable in terms of free energy as the cation valence increases but this stabilization saturates beyond the value +4 [165].

The efficacy of gene transfection into cells depends upon a large number of variables and to date no clear picture has been drawn relatively to the requirements for an optimal delivery of genes. It is commonly admitted that lipoplexes are internalized by endocytosis after binding to the negatively-charged cell surface thanks to their cationic charge [166]. The charge may also play a role in promoting the fusion necessary to escape the endosome. However, at high lipid-to-DNA charge ratio, the DNA may be so strongly coupled to the lipids that it cannot be released toward the nucleus [167]. The liquid-crystalline structure appears to be critical for an efficient release of DNA. A good configuration seems to start from a stable lamellar L_α^C lipoplex, which turns into a non-lamellar – possibly non-complexed hexagonal or cubic phase – upon mixing with the anionic lipids of the endosomal membrane [168,169].

4.2 Other lipid-polyelectrolyte complexes

Mixtures of cationic and neutral lipids that yield membranes in lamellar phase have been used in association with negatively-charged filamentous bacteriophage M13 virus and cytoskeletal filamentous actin (F-actin). The two polyelectrolytes have similar diameters, ~6.5 nm for the former and 7.5 nm for the latter, but different surface charge densities, 1 e^-/256 Å^2 and 1 e^-/625 Å^2 respectively. Like DNA, M13 virus and lipids form a complexed lamellar phase L_α^C with an inter-M13 spacing of 8.2 nm, slightly larger than the diameter of the M13 virus [170]. In contrast, F-actin and lipids result in the formation of ribbon-like nanotube structures with an average width of 250 nm and length up to 100 μm, consisting of lipid bilayers sandwiched between two layers of actin [171]. This difference of structure is attributed to the charge-density-matching mechanism: because the F-actin lattice of low charge density cannot compensate the charge density of the lipid membrane (1 e^+/251 Å^2), the system self-assemble into a superlattice structure where one layer membrane is matched against two layers of F-actin.

Another unconventional complexed lamellar structure is produced with poly-L-glutamic acid (PGA) polypeptides. Small angle x-ray scattering data revealed a "pinched lamellar" structure where anionic PGA and cationic lipids formed localized pinched regions; in between, the adjacent quasi-neutral bilayers swelled into large pockets of water stabilized by hydration repulsion [172].

The final structure of lipid-polyelectrolyte complexes arises from the interplay of the electrostatic interactions, the spontaneous curvature c_0 and the mean curvature modulus κ of the lipid membrane, the polyelectrolyte itself being considered as rigid enough not to bend over length scale comparable to the liquid-crystalline periodicities. When the polyelectrolyte curvature is much higher than c_0, the complex ends up in either L_α^C or H_{II}^C phase. If the curvatures fall into the same range as is the case with negatively-charged microtubules (~26 nm in diameter), the lipids form either a beads-on-a-rod structure along the polyelectrolyte at $\kappa >> 10k_BT$, or at low κ ($< 10k_BT$), they wrap it up in a bilayer to make a templated nanotube (Figure 11) [173-175].

4.3 Association with inorganic materials

Lipid bilayers immobilized on solid supports have become very popular for mimicking the basic processes occurring on a real cell membrane (see the section dedicated to raft microdomains) and for biotechnological applications [176,177]. A number of coupling techniques have been developed over the past decades including polymer-cushioned lipid bilayers [178,179], hybrid bilayers [180], tethered lipid bilayers [181] and physically self-assembled lipid monolayers [182], with the possibility to pattern the membranes on the micron scale by using photolithography [183]. The simplest route though is by the spreading of small lipid vesicles on hydrophilic substrates [184], employing if necessary divalent cations to bridge the like charges of lipids and substrate [185,186].

In nanotechnology, the association of lipids with carbon nanotubes aims at functionalizing inorganic nanoobjects for bio-related applications. Carbon nanotubes are tubular assemblies of carbon atoms with inner diameters ranging from 1 to 10 nm and possess a number of attractive mechanical and electrical properties [187]. Intrinsically hydrophobic, they are poorly soluble in aqueous solution. Synthetic single-chain lipids designed for the immobilization of histidine-tagged proteins can successfully coat carbon nanotubes in monolayer [188]. Lysophospholipids, i.e. single-chained phospholipids, form striated arrangements with a ~4.5-nm periodicity [189] on the surface of single-walled carbon nanotubes (Figure 12), and improve dramatically their solubility [190]. Lipid bilayers can be also obtained around nanotubes by coating them with layers of oppositely charged flexible polyelectrolytes prior to liposome fusion [191]. These systems are anticipated to yield novel sensors, biosensors and photo-switched functional devices [192], and may be used for nanotoxicological studies [193].

5. Perspectives on computer simulations

Most of the studies described above relied on experimental methodologies to get structural information about the system of interest, often indirectly. Electron microscopy, x-ray scattering, atomic force microscopy, all these techniques give only certain features of the structure – symmetry or periodicity -, and must be supplemented with careful interpretations to reconstruct the detailed arrangement. The prediction of the final structure for a given system is challenging

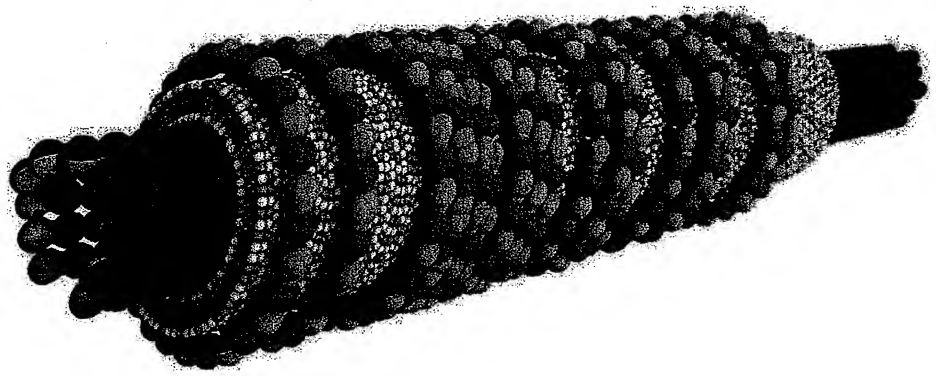

Figure 11
Lipid-microtubule nanotube. Complexed nanotube consisting of a microtubule (~26 nm in diameter) made of tubulin protein subunits (red-blue-yellow-green spheres) coated by a cationic lipid bilayer (headgroups in green and white, hydrocarbon tails in yellow). A third layer of tubulin oligomers actually wraps up the bilayer in the plane perpendicular to the nanotube axis. The arrangement is deduced from x-ray data and transmission electron microscopy images. Reproduced from reference [175] with permission. Copyright 2007 by the Biophysical Society.

because a huge number of molecular interactions usually come into play. With the refinement of statistical mechanics models and the increasing rapidity of modern computers, fine structural calculations and dynamic over long time scale become accessible, for system complexity up to a limited extent though. We shall give a few words about the possibilities offered by computational techniques to self-assembled lipidic systems.

A lot of the underlying physics can be obtained by phenomenological Hamiltonians which conceive of the lipid systems as an assembly of thin interfaces characterized by their elastic constants. This description permits to deal with large systems, considering the collective behavior of

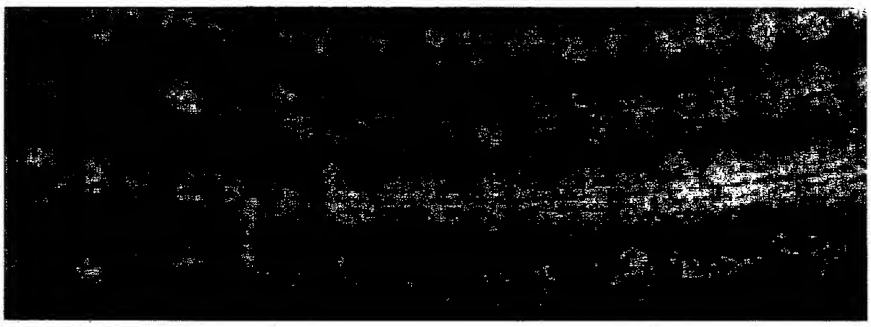

Figure 12
Lipid bilayers templated on carbon nanotubes. Transmission electron microscopy image of self-assembled single-chained lysophospholipids on single-walled carbon nanotubes. The assemblies display a striation periodicity of ~4.5 nm. The scale bar is 15 nm. Reproduced from reference [189] with permission. Copyright 2006 by the American Chemical Society.

lipid molecules possibly in interaction with polyelectrolytes. It is a very convenient approach to predict the equilibrium shape adopted by exotic vesicles [111]. We can also calculate the complete phase diagram of cationic lipid-DNA complexes as a function of the lipid composition and the lipid-to-DNA charge ratio [194,195]. This method, easy to implement numerically, yet requires an *a priori* knowledge of the system and of its behavior through the choice of suitable parameters. Density-Functional Theory (DFT) proceeds in a similar way, namely by assuming that the organized structures satisfy a local minimum of the free energy, this latter being represented in terms of molecular density-functionals [196,197]. Based on coarse-grained models of lipid molecules, DFT is able to reconstruct the phase diagram of lipid bilayers, predicting the transition from dilute bilayers to lamellar phase [198]. Applied to self-assembled systems, DFT is still in its infancy but holds many promises as it provides a rather fine structural description at a low computational cost.

A step further toward the real life is achieved by coarse-grained models implemented in Monte Carlo or molecular dynamic computer schemes [199,200]. In these models, group of atoms are lumped into pseudo-particles interacting via pair potentials. Noticeably, models with implicit solvent, in which hydrophilic/hydrophobic interactions are heuristically embedded into the pair potentials without the mediation of solvent molecules, enable to simulate large self-assembled lipidic systems with a decent accuracy and reasonable computational cost. They reproduce the elastic properties of weakly undulating lipid bilayers [201], as well as the self-assembly of lipid-DNA complexes [152,165,202]. Figure 13 shows a self-assembled lipid-ion-DNA complex in H_{II}^{C} phase simulated through a Monte Carlo scheme. Such a simple simulation gives quantitatively access to the thermodynamical stability of complexes in function of the valence of cations for instance. Other models, with explicit solvent, are able to reproduce the thermotropic lamellar-to-hexagonal phase transition of unsaturated phospholipids [203] or the two-dimensional phase separation occurring on the surface of binary fluid vesicles [204].

The ultimate refinement in molecular simulation is achieved by atomistic models in which the molecular structure and the interactions of components are described faithfully, including chemical bonds (bond, angle and dihedral potentials), electrostatic and van der Waals interactions [205]. Extremely accurate, they cannot, however, deal comfortably with mesoscale systems (extending beyond 10 nm) or track most of the self-assembly processes taking place beyond microseconds given the insufficient power of nowadays computers. Atomistic models have been up to now well suited for investigating the atomic interactions between lipids and proteins [206], lipids and DNA [207], or the configuration of lipids sticking around carbon nanotube [189], from a pre-assembled system close to its equilibrium, but they might reveal themselves as the method of choice for unraveling the full dynamic of self-assembly processes at atomic scale as soon as the computer technology will allow it.

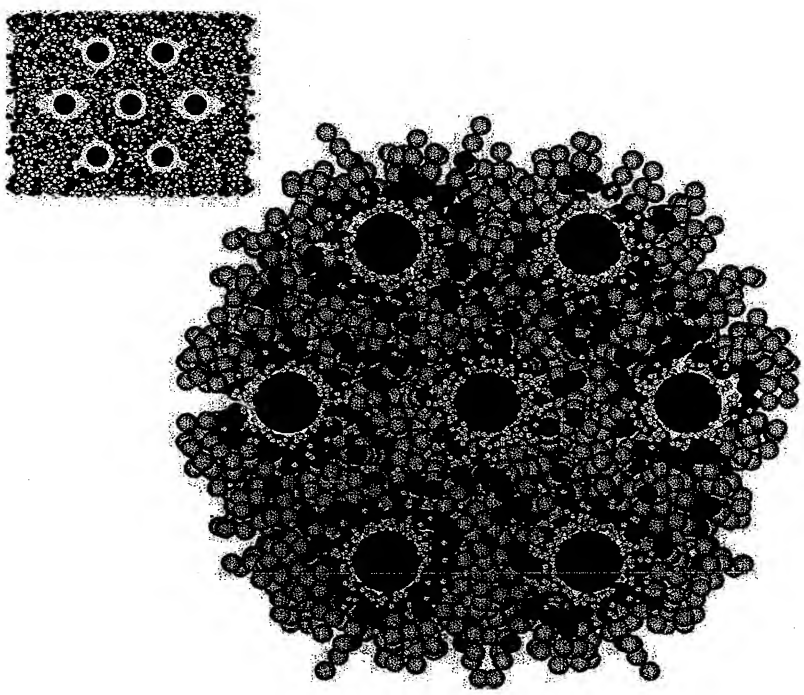

Figure 13
Computer simulation of a self-assembled lipidic complex. This water-free Monte Carlo simulation represents a hexagonal complex of zwitterionic lipids (headgroups in red and hydrocarbon chains in grey), divalent cations (yellow spheres) and DNA rods (blue). The DNA rods are maintained fixed on a hexagonal lattice over the simulation. Lipids and cations are randomly distributed at the initial stage (inset). Reproduced from reference [165] with permission. Copyright 2007 by the American Chemical Society.

6. Conclusion

This short review has shown the diversity, the complexity and the multiscale nature of lipidic systems, no matter if they are purely made of lipids or in association with polyelectrolytes and inorganic materials. Figure 14 summarizes the various lipidic structures described before. When the packing parameter of lipids p is larger than 1 or smaller than 0.5, the system tends to form non-lamellar phases such as hexagonal and cubic phases. Otherwise ($1/2 < p < 1$), lamellar phases are obtained, with lipids in fluid or gel state depending on their phase transition temperature. Upon mixing lipids in different state, segregation into raft microdomains occurs. At the macroscopic scale, lamellar membranes form spontaneously spherical vesicles, or exhibit other shapes (tube, starfish, prolate etc.) when submitted to a constraint such as a difference of osmotic pressure between the interior of the vesicle and the bulk solution. In the presence of another material presenting a favorable electrostatic interaction with the lipids, three other structures are achieved depending on c_0, the local curvature of the material C_M, and the mean curvature modulus of lipid membrane κ. At high material curvature $C_M >> C_0$, complexed phases are generally obtained (L_α^C ,

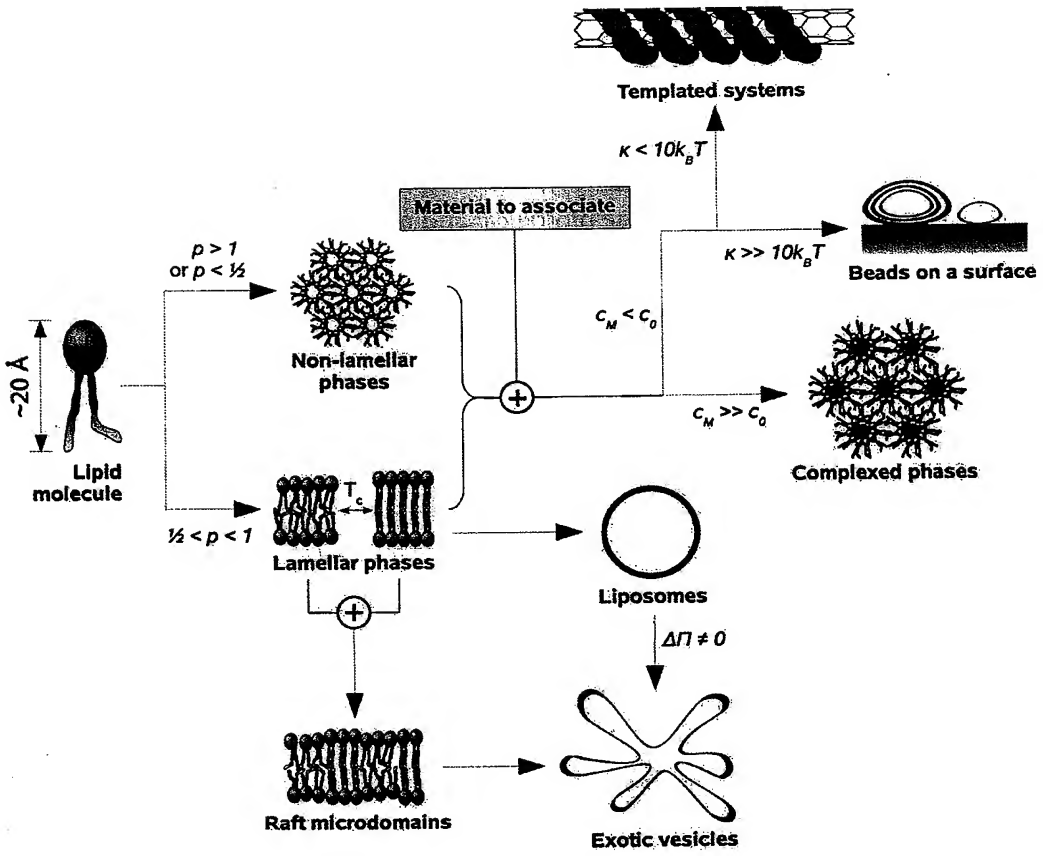

Figure 14

Overview of the structures formed by self-assembled lipidic systems. The structures described in this mini-review are summarized along with the physical factors enabling to get from one structural category to another. p denotes the lipid packing parameter, c_0 and κ are the spontaneous curvature and the mean curvature modulus of membranes, T_c is the critical temperature of lipid phase transition, $\Delta\Pi$ is the difference of osmotic pressure between the interior of vesicles and the bulk solution, and C_M stands for the local curvature of a material to associate. Each structural category is illustrated by a schematic of a typical lipidic structure: inverted hexagonal phase H_{II}, fluid and gel lamellar phases L_α and L_β, raft microdomains, liposomes and starfish vesicles, complexed inverted hexagonal phase H_{II}^C, lipid vesicles on a surface, and lipid-coated carbon nanotubes.

H_{II}^C etc.). If now the membrane curvature is higher than that of the material, either lipid vesicles with a stiff membrane ($\kappa >> 10k_B T$) are immobilized on the material surface, or the lipid membrane is flexible enough ($\kappa > 10k_B T$) to coat the material and results in a templated system.

If Biology finds naturally more interest in active compounds, that is, proteins and enzymes with dynamic and vital functions to the cell, Physics still remains intrigued and inquiring about

the fundamental principles that drive the lipid self-organization into mesoscale structures covering three orders of magnitude in the nanometer range. Not only lipids may tell us about the spark that gave birth to primitive living organisms – Life is after all, a self-assembly process -, but also, by harnessing the building blocks of Life, we may be able to mimic, or even trick, Nature, and design Life-like systems performing specific tasks in a better way. No matter what the applications may be, protein crystallization or gene delivery, it is a safe bet that understanding self-assembled lipidic systems will continue to enrich the biological and medical research.

Acknowledgements

Several figures were prepared with the POV-Ray raytracer package http://www.povray.org. This study was supported by the Agency for Science, Technology and Research (A*STAR) in Singapore.

References

1. Alberts B, Johnson A, Lewis J, Raff M, Roberts K, Walter P: *Molecular biology of the cell. Garland Science, New York* 2002.
2. Luecke H, Richter HT, Lanyi JK: *Science* 1998, **280**:1934-1937.
3. Alber F, Dokudovskaya S, Veenhoff LM, Zhang W, Kipper J, Devos D, Suprapto A, Karni-Schmidt O, Williams R, Chait BT, Sali A, Rout MP: *Nature* 2007, **450**:695-701.
4. Alber F, Dokudovskaya S, Veenhoff LM, Zhang W, Kipper J, Devos D, Suprapto A, Karni-Schmidt O, Williams R, Chait BT, Rout MP, Sali A: *Nature* 2007, **450**:683-694.
5. Rondelez Y, Tresset G, Nakashima T, Kato-Yamada Y, Fujita H, Takeuchi S, Noji H: *Nature* 2005, **433**:773-777.
6. Boyer PD: *Annu Rev Biochem* 1997, **66**:717-749.
7. Mahfoud R, Garmy N, Maresca M, Yahi N, Puigserver A, Fantini J: *J Biol Chem* 2002, **277**:11292-11296.
8. Smith DC, Lord JM, Roberts LM, Johannes L: *Semin Cell Dev Biol* 2004, **15**:397-408.
9. Sandvig K, Spilsberg B, Lauvrak SU, Torgersen ML, Iversen T, van Deurs B: *Int J Med Microbiol* 2004, **293**:483-490.
10. Hunter RJ: *Foundations of colloid science* Oxford University Press, New York; 2001.
11. Gelbart WM, Ben-Shaul A: *J Phys Chem* 1996, **100**:13169-13189.
12. Israelachvili J: *Intermolecular and surface forces* Academic Press; 1991.
13. Tanford C: *The hydrophobic effect. Formation of micelles and biological membranes* Wiley, New York; 1980.
14. Willard AP, Chandler D: *J Phys Chem B* 2008, **112**:6187-6192.
15. Chandler D: *Nature* 2005, **437**:640-647.
16. Despa F, Berry RS: *Biophys J* 2007, **92**:373-378.
17. Meyer EE, Rosenberg KJ, Israelachvili J: *Proc Natl Acad Sci USA* 2006, **103**:15739-15746.
18. Maibaum L, Dinner AR, Chandler D: *J Phys Chem B* 2004, **108**:6778-6781.
19. Israelachvili JN, Mitchell DJ, Ninham BW: *J Chem Soc Faraday Trans 2* 1976, **72**:1525-1568.
20. Zemb T, Dubois M, Deme B, Gulik-Krzywicki T: *Science* 1999, **283**:816-819.
21. Dubois M, Lizunov V, Meister A, Gulik-Krzywicki T, Verbavatz JM, Perez E, Zimmerberg J, Zemb T: *Proc Natl Acad Sci USA* 2004, **101**:15082-15087.
22. Dubois M, Demé B, Gulik-Krzywicki T, Dedieu JC, Vautrin C, Désert S, Perez E, Zemb T: *Nature* 2001, **411**:672-675.
23. Gonzalez-Pérez A, Schmutz M, Waton G, Romero MJ, Krafft MP: *J Am Chem Soc* 2007, **129**:756-757.
24. Ulrich AS: *Biosci Rep* 2002, **22**:129-150.
25. Lasic DD: *Trends Biotechnol* 1998, **16**:307-321.
26. Karlsson M, Davidson M, Karlsson R, Karlsson A, Bergenholtz J, Konkoli Z, Jesorka A, Lobovkina T, Hurtig J, Voinova M, Orwar O: *Annu Rev Phys Chem* 2004, **55**:613-649.
27. Jesorka A, Orwar O: *Annu Rev Anal Chem* 2008, **1**:801-832.
28. Liang H, Angelini TE, Ho J, Braun PV, Wong GCL: *J Am Chem Soc* 2003, **125**:11786-11787.
29. Menger FM, Chlebowski ME, Galloway AL, Lu H, Seredyuk VA, Sorrells JL, Zhang H: *Langmuir* 2005, **21**:10336-10341.
30. Olmsted PD: **Self-assembly and properties of lipid membranes.** In *Soft condensed matter physics in molecular and cell biology* Edited by: Poon WCK, Andelman D. Taylor & Francis, Boca Raton; 2006:63-77.
31. Helfrich W: *Z Naturforsch [C]* 1973, **28**:693-703.
32. Kucerka N, Pencer J, Sachs JN, Nagle JF, Katsaras J: *Langmuir* 2007, **23**:1292-1299.
33. Pan J, Mills TT, Tristram-Nagle S, Nagle JF: *Phys Rev Lett* 2008, **100**:198103.
34. Pan J, Tristram-Nagle S, Kucerka N, Nagle JF: *Biophys J* 2008, **94**:117-124.
35. Daillant J, Bellet-Amalric E, Braslau A, Charitat T, Fragneto G, Graner F, Mora S, Rieutord F, Stidder B: *Proc Natl Acad Sci USA* 2005, **102**:11639-11644.
36. Koynova R, Caffrey M: *Biochim Biophys Acta* 1998, **1376**:91-145.
37. Sun WJ, Tristram-Nagle S, Suter RM, Nagle JF: *Proc Natl Acad Sci USA* 1996, **93**:7008-7012.
38. Pisani M, Bruni P, Caracciolo G, Caminiti R, Francescangeli O: *J Phys Chem B* 2006, **110**:13203-13211.
39. Tsong TY: *Biophys J* 1991, **60**:297-306.
40. Tresset G, Iliescu C: *Appl Phys Lett* 2007, **90**:173901.
41. Olofsson J, Nolkrantz K, Ryttsén F, Lambie BA, Weber SG, Orwar O: *Curr Opin Biotechnol* 2003, **14**:29-34.
42. de Almeida RFM, Fedorov A, Prieto M: *Biophys J* 2003, **85**:2406-2416.
43. Jain MK, White HB: *Adv Lipid Res* 1977, **15**:1-60.
44. Klausner RD, Kleinfeld AM, Hoover RL, Karnovsky MJ: *J Biol Chem* 1980, **255**:1286-1295.
45. Edidin M: *Annu Rev Biophys Biomol Struct* 2003, **32**:257-283.
46. Munro S: *Cell* 2003, **115**:377-388.
47. Helms JB, Zurzolo C: *Traffic* 2004, **5**:247-254.
48. Allen JA, Halverson-Tamboli RA, Rasenick MM: **L.** *Nat Rev Neurosci* 2007, **8**:128-140.

49. Fantini J, Garmy N, Mahfoud R, Yahi N: *Expert Rev Mol Med* 2002, **4**:1-22.
50. Hebbar S, Lee E, Manna M, Steinert S, Kumar GS, Wenk M, Wohland T, Kraut R: *J Lipid Res* 2008, **49**:1077-1089.
51. Steinert S, Lee E, Tresset G, Zhang D, Hortsch R, Wetzel R, Hebbar S, Sundram JR, Kesavapany S, Boschke E, Kraut R: *PLoS ONE* 2008, **3**:e2933.
52. Henderson RM, Edwardson JM, Geisse NA, Saslowsky DE: **Lipid rafts: feeling is believing.** *News Physiol Sci* 2004, **19**:39-43.
53. Burns AR, Frankel DJ, Buranda T: *Biophys J* 2005, **89**:1081-1093.
54. Shaw JE, Epand RF, Epand RM, Li Z, Bittman R, Yip CM: *Biophys J* 2006, **90**:2170-2178.
55. Chiantia S, Kahya N, Ries J, Schwille P: *Biophys J* 2006, **90**:4500-4508.
56. Lin W, Blanchette CD, Ratto TV, Longo ML: **Lipid domains in supported lipid bilayer for atomic force microscopy.** In *Methods in membrane lipids* Edited by: Dopico AM. Humana Press, Totowa; 2007:503-513.
57. Johnston LJ: *Langmuir* 2007, **23**:5886-5895.
58. Bernardino de la Serna J, Perez-Gil J, Simonsen AC, Bagatolli LA: *J Biol Chem* 2004, **279**:40715-40722.
59. Yethiraj A, Weisshaar JC: *Biophys J* 2007, **93**:3113-3119.
60. Lingwood D, Ries J, Schwille P, Simons K: *Proc Natl Acad Sci USA* 2008, **105**:10005-10010.
61. Kaasgaard T, Drummond CJ: *Phys Chem Chem Phys* 2006, **8**:4957-4975.
62. Luzzati V, Tardieu A: *Annu Rev Phys Chem* 1974, **25**:79-94.
63. Luzzati V, Husson F: *J Cell Biol* 1962, **12**:207-219.
64. Luzzati V, Reiss-Husson F, Rivas E, Gulik-Krzywicki T: *Ann New York Acad Sci* 1966, **137**:409-413.
65. Seddon JM: *Biochim Biophys Acta* 1990, **1031**:1-69.
66. Koynova R, Caffrey M: *Chem Phys Lipids* 1994, **69**:1-34.
67. Turner DC, Gruner SM: *Biochemistry* 1992, **31**:1340-1355.
68. Kozlov MM, Leikin S, Rand RP: *Biophys J* 1994, **67**:1603-1611.
69. Gawrisch K, Parsegian VA, Hajduk DA, Tate MW, Graner SM, Fuller NL, Rand RP: *Biochemistry* 1992, **31**:2856-2864.
70. Siegel DP: *Biophys J* 1999, **76**:291-313.
71. Siegel DP, Kozlov MM: *Biophys J* 2004, **87**:366-374.
72. Luzzati V: *Curr Opin Struct Biol* 1997, **7**:661-668.
73. Seddon JM, Robins J, Gulik-Krzywicki T, Delacroix H: *Phys Chem Chem Phys* 2000, **2**:4485-4493.
74. Charvolin J, Sadoc J: *Phil Trans R Soc Lond A* 1996, **354**:2173-2192.
75. Barauskas J, Johnsson M, Tiberg F: *Nano Lett* 2005, **5**:1615-1619.
76. Johnsson M, Barauskas J, Tiberg F: *J Am Chem Soc* 2005, **127**:1076-1077.
77. Barauskas J, Misiunas A, Gunnarsson T, Tiberg F, Johnsson M: *Langmuir* 2006, **22**:6328-6334.
78. Seddon JM: *Biochemistry* 1990, **29**:7997-8002.
79. Luzzati V, Gambacorta A, DeRosa M, Gulik A: *Annu Rev Biophys Biophys Chem* 1987, **16**:25-47.
80. Landh T: *FEBS Lett* 1995, **369**:13-17.
81. Landau EM, Rosenbusch JP: *Proc Natl Acad Sci USA* 1996, **93**:14532-14535.
82. Caffrey M: *Curr Opin Struct Biol* 2000, **10**:486-497.
83. Cherezov V, Rosenbaum DM, Hanson MA, Rasmussen SGF, Thian FS, Kobilka TS, Choi H, Kuhn P, Weis WI, Kobilka BK, Stevens RC: *Science* 2007, **318**:1258-1265.
84. Bangham AD, Horne RW: *J Mol Biol* 1964, **8**:660-668.
85. Lasic DD: **Giant vesicles: a historical introduction.** In *Giant vesicles* Edited by: Luisi PL, Walde P. John Wiley & Sons, Chichester; 2000:11-24.
86. Segota S, Tezak D: *Adv Colloid Interface Sci* 2006, **121**:51-75.
87. Torchilin VP, Weissig V: *Liposomes* Oxford University Press, Oxford; 2003.
88. Voinea M, Simionescu M: *J Cell Mol Med* 2002, **6**:465-474.
89. Vasir JK, Reddy MK, Labhasetwar VD: *Curr Nanosci* 2005, **1**:47-64.
90. Lian T, Ho RJY: *J Pharm Sci* 2001, **90**:667-680.
91. Karanth H, Murthy RSR: *J Pharm Pharmacol* 2007, **59**:469-483.
92. Park YS: *Biosci Rep* 2002, **22**:267-281.
93. Allen C, Dos Santos N, Gallagher R, Chiu GNC, Shu Y, Li WM, Johnstone SA, Janoff AS, Mayer LD, Webb MS, Bally MB: *Biosci Rep* 2002, **22**:225-250.
94. Mason JT, Xu L, Sheng Z, O'Leary TJ: *Nat Biotechnol* 2006, **24**:555-557.
95. Mason JT, Xu L, Sheng Z, He J, O'Leary TJ: *Nat Protoc* 2006, **1**:2003-2011.
96. Kremer JJ, Murphy RM: *J Biochem Biophys Methods* 2003, **57**:159-169.
97. Chan YM, Boxer SG: *Curr Opin Chem Biol* 2007, **11**:581-587.
98. Stoicheva NG, Hui SW: *Biochim Biophys Acta* 1994, **1195**:31-38.
99. Tresset G, Takeuchi S: *Anal Chem* 2005, **77**:2795-2801.
100. Tresset G, Takeuchi S: *Biomed Microdevices* 2004, **6**:213-218.
101. Dimova R, Riske KA, Aranda S, Bezlyepkina N, Knorr RL, Lipowsky R: *Soft Matter* 2007, **3**:817-827.
102. Riquelme G, Lopez E, Garcia-Segura LM, Ferragut JA, Gonzalez-Ros JM: *Biochemistry* 1990, **29**:11215-11222.
103. Karlsson A, Sott K, Markström M, Davidson M, Konkoli Z, Orwar O: *J Phys Chem B* 2005, **109**:1609-1617.
104. Sott K, Lobovkina T, Lizana L, Tokarz M, Bauer B, Konkoli Z, Orwar O: *Nano Lett* 2006, **6**:209-214.
105. Nomura SM, Tsumoto K, Hamada T, Akiyoshi K, Nakatani Y, Yoshikawa K: *Chembiochem* 2003, **4**:1172-1175.
106. Noireaux V, Libchaber A: *Proc Natl Acad Sci USA* 2004, **101**:17669-17674.
107. Ishikawa K, Sato K, Shima Y, Urabe I, Yomo T: *FEBS Lett* 2004, **576**:387-390.
108. Hotani H: *J Mol Biol* 1984, **178**:113-120.
109. Käs J, Sackmann E: *Biophys J* 1991, **60**:825-844.
110. Miao L, Seifert U, Wortis M, Döbereiner H: *Phys Rev E Stat Phys Plasmas Fluids Relat Interdiscip Topics* 1994, **49**:5389-5407.
111. Seifert U: *Adv Phys* 1997, **46**:13-137.
112. Ziherl P, Svetina S: *Europhys Lett* 2005, **70**:690-696.
113. Michalet X: *Phys Rev E Stat Nonlin Soft Matter Phys* 2007, **76**:021914.
114. Yanagisawa M, Imai M, Taniguchi T: *Phys Rev Lett* 2008, **100**:148102.
115. Jülicher F, Lipowsky R: *Phys Rev E Stat Phys Plasmas Fluids Relat Interdiscip Topics* 1996, **53**:2670-2683.
116. Baumgart T, Das S, Webb WW, Jenkins JT: *Biophys J* 2005, **89**:1067-1080.
117. Harden JL, Mackintosh FC, Olmsted PD: *Phys Rev E Stat Nonlin Soft Matter Phys* 2005, **72**:011903.
118. Sens P, Turner MS: *Phys Rev E Stat Nonlin Soft Matter Phys* 2006, **73**:031918.

119. Korlach J, Schwille P, Webb WW, Feigenson GW: *Proc Natl Acad Sci USA* 1999, **96**:8461-8466.
120. Baumgart T, Hess ST, Webb WW: *Nature* 2003, **425**:821-824.
121. Bagatolli LA, Gratton E: *Biophys J* 2000, **78**:290-305.
122. Veatch SL, Keller SL: *Biophys J* 2003, **85**:3074-3083.
123. Ariola FS, Mudaliar DJ, Walvick RP, Heikal AA: *Phys Chem Chem Phys* 2006, **8**:4517-4529.
124. Yanagisawa M, Imai M, Masui T, Komura S, Ohta T: *Biophys J* 2007, **92**:115-125.
125. Sesso A, de Faria FP, Iwamura ES, Corrêa H: *J Cell Sci* 1994, **107(Pt 3)**:517-528.
126. Sciaky N, Presley J, Smith C, Zaal KJ, Cole N, Moreira JE, Terasaki M, Siggia E, Lippincott-Schwartz J: *J Cell Biol* 1997, **139**:1137-1155.
127. Iglic A, Hagerstrand H, Bobrowska-Hagerstrand M, Arrigler V, Kraij-Iglic V: *Phys Lett A* 2003, **310**:493-497.
128. Shimizu T, Masuda M, Minamikawa H: *Chem Rev* 2005, **105**:1401-1443.
129. Shimizu T: *J Polym Sci Pol Chem* 2008, **46**:2601-2611.
130. Brazhnik KP, Vreeland WN, Hutchison JB, Kishore R, Wells J, Helmerson K, Locascio LE: *Langmuir* 2005, **21**:10814-10817.
131. Cuvelier D, Chiaruttini N, Bassereau P, Nassoy P: *Europhys Lett* 2005, **71**:1015-1021.
132. Tokarz M, Akerman B, Olofsson J, Joanny J, Dommersnes P, Orwar O: *Proc Natl Acad Sci USA* 2005, **102**:9127-9132.
133. Karlsson M, Davidson M, Karlsson R, Karlsson A, Bergenholtz J, Konkoli Z, Jesorka A, Lobovkina T, Hurtig J, Voinova M, Orwar O: *Annu Rev Phys Chem* 2004, **55**:613-649.
134. Mahajan N, Fang J: *Langmuir* 2005, **21**:3153-3157.
135. Liu H, Bachand GD, Kim H, Hayden CC, Abate EA, Sasaki DY: *Langmuir* 2008, **24**:3686-3689.
136. Schnur JM: *Science* 1993, **262**:1669-1676.
137. Thomas BN, Safinya CR, Plano RJ, Clark NA: *Science* 1995, **267**:1635-1638.
138. Zarif L: *J Control Release* 2002, **81**:7-23.
139. John G, Masuda M, Okada Y, Yase K, Shimizu T: *Adv Mater* 2001, **13**:715-718.
140. Frusawa H, Fukagawa A, Ikeda Y, Araki J, Ito K, John G, Shimizu T: *Angew Chem Int Ed* 2003, **42**:72-74.
141. Yui H, Guo Y, Koyama K, Sawada T, John G, Yang B, Masuda M, Shimizu T: *Langmuir* 2005, **21**:721-727.
142. Luo D, Saltzman WM: *Nat Biotechnol* 2000, **18**:33-37.
143. Allen TM, Cullis PR: *Science* 2004, **303**:1818-1822.
144. Gardlík R, Pálffy R, Hodosy J, Lukács J, Turna J, Celec P: *Med Sci Monit* 2005, **11**:RA110-21.
145. Mastrobattista E, Aa MAEM van der, Hennink WE, Crommelin DJA: *Nat Rev Drug Discov* 2006, **5**:115-121.
146. Rao NM, Gopal V: *Biosci Rep* 2006, **26**:301-324.
147. Desigaux L, Sainlos M, Lambert O, Chevre R, Letrou-Bonneval E, Vigneron J, Lehn P, Lehn J, Pitard B: *Proc Natl Acad Sci USA* 2007, **104**:16534-16539.
148. Felgner PL, Gadek TR, Holm M, Roman R, Chan HW, Wenz M, Northrop JP, Ringold GM, Danielsen M: *Proc Natl Acad Sci USA* 1987, **84**:7413-7417.
149. Lasic DD, Strey H, Stuart MCA, Podgornik R, Frederik PM: *J Am Chem Soc* 1997, **119**:832-833.
150. Rädler JO, Koltover I, Salditt T, Safinya CR: *Science* 1997, **275**:810-814.
151. Safinya CR: *Curr Opin Struct Biol* 2001, **11**:440-448.
152. Farago O, Ewert K, Ahmad A, Evans HM, Grønbech-Jensen N, Safinya CR: *Biophys J* 2008, **95**:836-846.
153. Koltover I, Wagner K, Safinya CR: *Proc Natl Acad Sci USA* 2000, **97**:14046-14051.
154. Caracciolo G, Pozzi D, Caminiti R, Mancini G, Luciani P, Amenitsch H: *J Am Chem Soc* 2007, **129**:10092-10093.
155. Koltover I, Salditt T, Rädler JO, Safinya CR: *Science* 1998, **281**:78-81.
156. Ewert KK, Evans HM, Zidovska A, Bouxsein NF, Ahmad A, Safinya CR: *J Am Chem Soc* 2006, **128**:3998-4006.
157. Hikita T, Tadano-Aritomi K, Iida-Tanaka N, Levery SB, Ishizuka I, Hakomori S: *Neurochem Res* 2002, **27**:575-581.
158. Dass CR: *J Mol Med* 2004, **82**:579-591.
159. Tatulian SA: **Surface electrostatics of biological membranes and ion binding.** In *Surface chemistry and electrochemistry of membranes* Edited by: Sørensen TS. Marcel Dekker, New York; 1999:872-922.
160. Francescangeli O, Stanic V, Gobbi L, Bruni P, Iacussi M, Tosi G, Bernstorff S: *Phys Rev E Stat Nonlin Soft Matter Phys* 2003, **67**:011904.
161. McManus JJ, Rädler JO, Dawson KA: *J Am Chem Soc* 2004, **126**:15966-15967.
162. Liang H, Harries D, Wong GCL: *Proc Natl Acad Sci USA* 2005, **102**:11173-11178.
163. Francescangeli O, Pisani M, Stani(V, Bruni P, Weiss TM: *Europhys Lett* 2004, **67**:669-675.
164. Tresset G, Cheong WCD, Tan YLS, Boulaire J, Lam YM: *Biophys J* 2007, **93**:637-644.
165. Tresset G, Cheong WCD, Lam YM: *J Phys Chem B* 2007, **111**:14233-14238.
166. Zuhorn IS, Engberts JBFN, Hoekstra D: *Eur Biophys J* 2007, **36**:349-362.
167. Ahmad A, Evans HM, Ewert K, George CX, Samuel CE, Safinya CR: *J Gene Med* 2005, **7**:739-748.
168. Koynova R, Wang L, Tarahovsky Y, MacDonald RC: *Bioconjug Chem* 2005, **16**:1335-1339.
169. Koynova R, Wang L, MacDonald RC: *Proc Natl Acad Sci USA* 2006, **103**:14373-14378.
170. Yang L, Liang H, Angelini TE, Butler J, Coridan R, Tang JX, Wong GCL: *Nat Mater* 2004, **3**:615-619.
171. Wong GC, Tang JX, Lin A, Li Y, Janmey PA, Safinya CR: *Science* 2000, **288**:2035-2039.
172. Subramanian G, Hjelm RP, Deming TJ, Smith GS, Li Y, Safinya CR: *J Am Chem Soc* 2000, **122**:26-34.
173. Raviv U, Needleman DJ, Li Y, Miller HP, Wilson L, Safinya CR: *Proc Natl Acad Sci USA* 2005, **102**:11167-11172.
174. Raviv U, Needleman DJ, Safinya CR: *J Phys-Condes Matter* 2006, **18**:1271-1279.
175. Raviv U, Nguyen T, Ghafouri R, Needleman DJ, Li Y, Miller HP, Wilson L, Bruinsma RF, Safinya CR: *Biophys J* 2007, **92**:278-287.
176. Sackmann E: *Science* 1996, **271**:43-48.
177. Sackmann E, Tanaka M: *Trends Biotechnol* 2000, **18**:58-64.
178. Goennenwein S, Tanaka M, Hu B, Moroder L, Sackmann E: *Biophys J* 2003, **85**:646-655.
179. Munro JC, Frank CW: *Langmuir* 2004, **20**:3339-3349.
180. Silin VI, Wieder H, Woodward JT, Valincius G, Offenhausser A, Plant AL: *J Am Chem Soc* 2002, **124**:14676-14683.
181. Purrucker O, Förtig A, Jordan R, Tanaka M: *Chemphyschem* 2004, **5**:327-335.
182. Phang T, Franses EI: *Langmuir* 2006, **22**:1609-1618.
183. Orth RN, Kameoka J, Zipfel WR, Ilic B, Webb WW, Clark TG, Craighead HG: *Biophys J* 2003, **85**:3066-3073.
184. Brian AA, McConnell HM: *Proc Natl Acad Sci USA* 1984, **81**:6159-6163.
185. Richter R, Mukhopadhyay A, Brisson A: *Biophys J* 2003, **85**:3035-3047.
186. Richter RP, Bérat R, Brisson AR: *Langmuir* 2006, **22**:3497-3505.

187. Tasis D, Tagmatarchis N, Bianco A, Prato M: *Chem Rev* 2006, **106**:1105-1136.
188. Richard C, Balavoine F, Schultz P, Ebbesen TW, Mioskowski C: *Science* 2003, **300**:775-778.
189. Qiao R, Ke PC: *J Am Chem Soc* 2006, **128**:13656-13657.
190. Wu Y, Hudson JS, Lu Q, Moore JM, Mount AS, Rao AM, Alexov E, Ke PC: *J Phys Chem B* 2006, **110**:2475-2478.
191. Artyukhin AB, Shestakov A, Harper J, Bakajin O, Stroeve P, Noy A: *J Am Chem Soc* 2005, **127**:7538-7542.
192. Ye J, Sheu F: *Curr Nanosci* 2006, **2**:319-327.
193. Ke PC: *Phys Chem Chem Phys* 2007, **9**:439-447.
194. May S, Ben-Shaul A: *Biophys J* 1997, **73**:2427-2440.
195. May S, Harries D, Ben-Shaul A: *Biophys J* 2000, **78**:1681-1697.
196. Wu J: *AIChE* 2006, **52**:1169-1193.
197. Wu J, Li Z: *Annu Rev Phys Chem* 2007, **58**:85-112.
198. Frink LJD, Frischknecht AL: *Phys Rev E Stat Nonlin Soft Matter Phys* 2005, **72**:041923.
199. Müller M, Katsov K, Schick M: *Phys Rep* 2006, **434**:113-176.
200. Venturoli M, Sperotto MM, Kranenburg M, Smit B: *Phys Rep* 2006, **437**:1-54.
201. Farago O: *J Chem Phys* 2003, **119**:596-605.
202. Farago O, Grønbech-Jensen N: *Biophys J* 2007, **92**:3228-3240.
203. Marrink S, Mark AE: *Biophys J* 2004, **87**:3894-3900.
204. Laradji M, Sunil Kumar PB: *J Chem Phys* 2005, **123**:224902.
205. Lu DY, Aksimentiev A, Shih AY, Cruz-Chu E, Freddolino PL, Arkhipov A, Schulten K: *Phys Biol* 2006, **3**:S40-S53.
206. Aksimentiev A, Schulten K: *Biophys J* 2005, **88**:3745-3761.
207. Bandyopadhyay S, Tarek M, Klein ML: *J Phys Chem B* 1999, **103**:10075-10080.

Fig.1. *PMC Biophysics* 2009, **2**:3, 1757-5036. Figure 3

The "hexagonal structure" is not spherical but cylindrical.

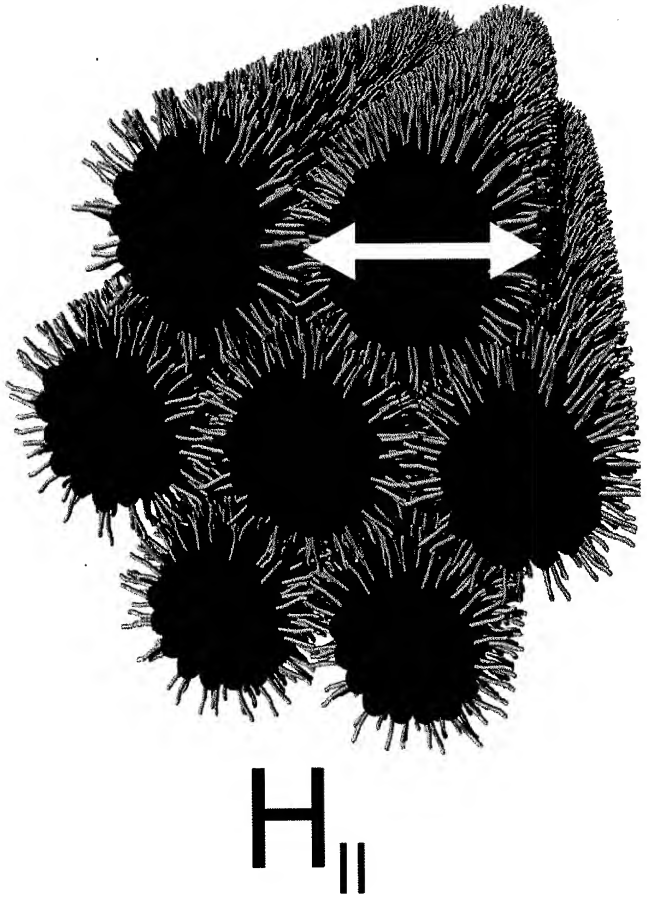

Fig. 2

Image by optical microscope, viewed from directly above.

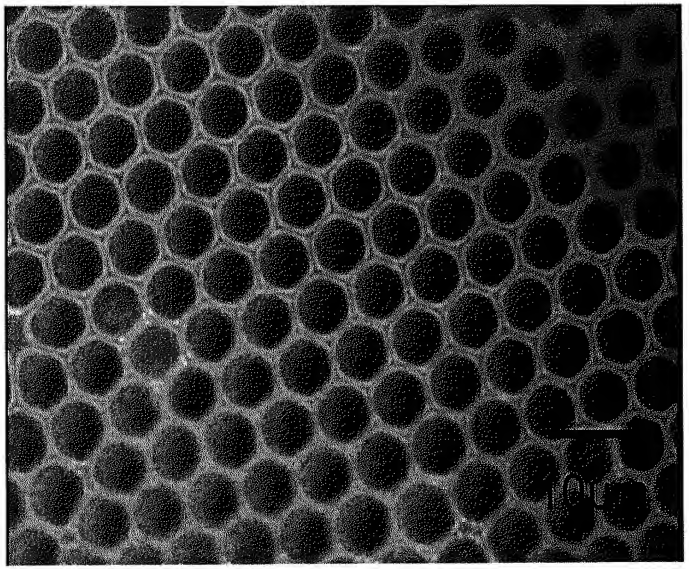

Image by SEM, cross-sectional view.

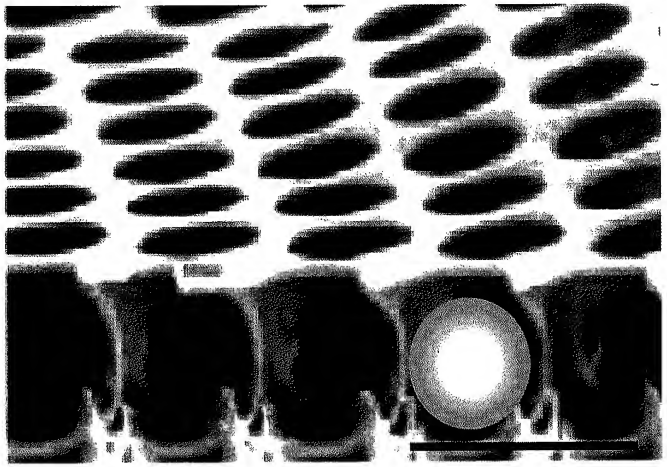

Honeycomb structure is formed by spherical droplet of water.

Schematic

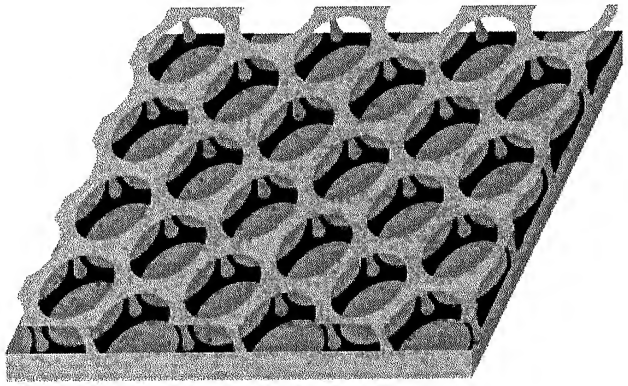

A hole is connected to adjacent six holes on the side to form continuous hole.

Reference Material 2

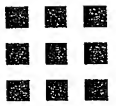

Intermolecular and Surface Forces

Third Edition

Jacob N. Israelachvili
UNIVERSITY OF CALIFORNIA
SANTA BARBARA, CALIFORNIA, USA

ELSEVIER

AMSTERDAM • BOSTON • HEIDELBERG • LONDON • NEW YORK • OXFORD
PARIS • SAN DIEGOSAN FRANCISCO • SINGAPORE • SYDNEY • TOKYO

Academic Press is an imprint of Elsevier

The simple hard and soft packing models developed so far takes us about as far as one can go without resorting to much more sophisticated theoretical methods in which the various intermolecular and interaggregate interactions are treated to a full statistical thermodynamic analysis or a computer simulation. These have been done for micelles (Jönsson and Wennerström, 1981; Gruen, 1985; Szleifer et al., 1985, 1986; Jokela et al., 1987; Blanckstein et al., 1986) and bilayers (Leermakers and Scheutjens, 1988; Egberts and Berendsen, 1988; Cevc and Marsh, 1987; De Loof et al., 1991; Stevens, 2003). Even more complex structures are considered in the next Section.

20.9 Other Amphiphilic Structures and the Transitions between Them

We have seen that the geometric packing properties of different lipids may be conveniently expressed in terms of the packing parameter $v/a_0\ell_c$ characteristic for each lipid in a given solution environment, the value of which determines the type of aggregate formed. Table 20.3 illustrates the structures formed by some common surfactants and lipids, and how these can be modified by their ionic environment, temperature, chain unsaturation, and so on, as will now be summarized (see also Figure 20.3).

1. **Factors affecting headgroup area.** Lipids with smaller headgroup areas (high $v/a_0\ell_c$) form larger vesicles, less-curved bilayers, or inverted micellar phases. For anionic headgroups, this can be brought about by increasing the salt concentration, particularly Ca^{2+} or lowering the pH. This also has the effect of straightening (condensing) the chains.
2. **Factors affecting chain packing.** Introducing chain branching and unsaturation, particularly of cis double bonds, reduces ℓ_c and thus increases $v/a_0\ell_c$. Similar effects occur when the effective volume, v, of the chains is increased due to the penetration of organic molecules such as low MW alkanes into the chain regions. Both of the preceding effects lead to larger vesicles and ultimately to inverted structures. In the case of microemulsions (surfactant/water/oil mixtures), they lead to larger oil-in-water droplets and ultimately to inverted water-in-oil droplets (Figure 20.9).
3. **Effects of temperature *T*.** The effects of temperature are more subtle and generally less well understood. The areas of more hydrophilic headgroups usually increase with T due to the increased steric repulsion between them, and this acts to decrease $v/a_0\ell_c$. Thus, with increasing temperature charged micelles usually shrink (Missel et al., 1980). But spherical micelles of nonionic surfactants grow and become more cylindrical, probably due to the reduced repulsion between the headgroups with increasing T (see Figure 21.10). Zwitterionic micelles appear to behave somewhere in between, and their aggregation numbers hardly change with temperature (Malliaris et al., 1985).
4. **Lipid mixtures.** When an aggregate is composed of a lipid mixture, as long as the different molecules mix ideally and do not phase-separate, the aggregate properties may be treated, in a first approximation, in terms of some mean packing parameter

Table 20.3 Mean (Dynamic) Packing Shapes of Lipids and the Structures They Form†

Lipid	Critical packing parameter $v/a_0\ell_c$	Critical packing shape	Structures formed
Single-chained lipids (surfactants) with large head-group areas: *SDS in low salt*	< 1/3	Cone 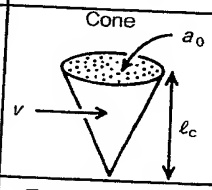	Spherical micelles 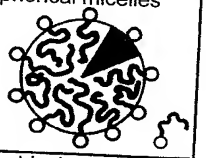
Single-chained lipids with small head-group areas: *SDS and CTAB in high salt, nonionics*	1/3–1/2	Truncated cone 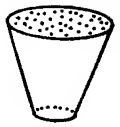	Cylindrical micelles 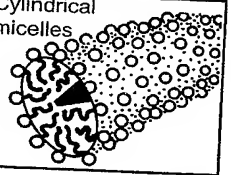
Double-chained lipids with large head-group areas, fluid chains: *Phosphatidyl choline (lecithin), Phosphatidyl serine, Phosphatidyl glycerol, Phosphatidyl inositol, Phosphatidic acid, sphingomyelin, DGDG[a], dihexadecyl phosphate, dialkyl dimethyl ammonium salts*	1/2–1	Truncated cone 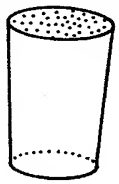	Flexible bilayers, vesicles 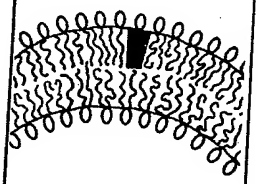
Double-chained lipids with small head-group areas, anionic lipids in high salt, saturated frozen chains: *phosphatidyl ethanolamine, phosphatidyl serine + Ca^{2+}*	~1	Cylinder 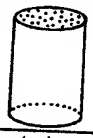	Planar bilayers 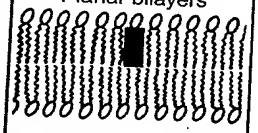
Double-chained lipids with small head-group areas, nonionic lipids, poly *(cis)* unsaturated chains, high T: *unsat. phosphatidyl ethanolamine, cardiolipin + Ca^{2+} phosphatidic acid + Ca^{2+} cholesterol, MGDG[b]* ←	>1	Inverted truncated cone or wedge 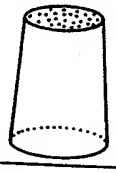	Inverted micelles 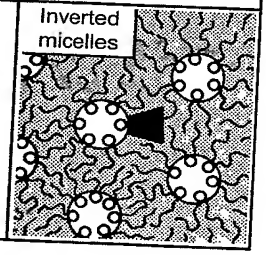

[a]DGDG, digalactosyl diglyceride, diglucosyl diglyceride.
[b]MGDG, monogalactosyl diglyceride, monoglucosyl diglyceride.

†Fluorocarbon chains are more rigid than hydrocarbon chains. Consequently, fluorocarbon surfactants form less curved structures, and often assembly only into planar bilayers.

Fig. 3

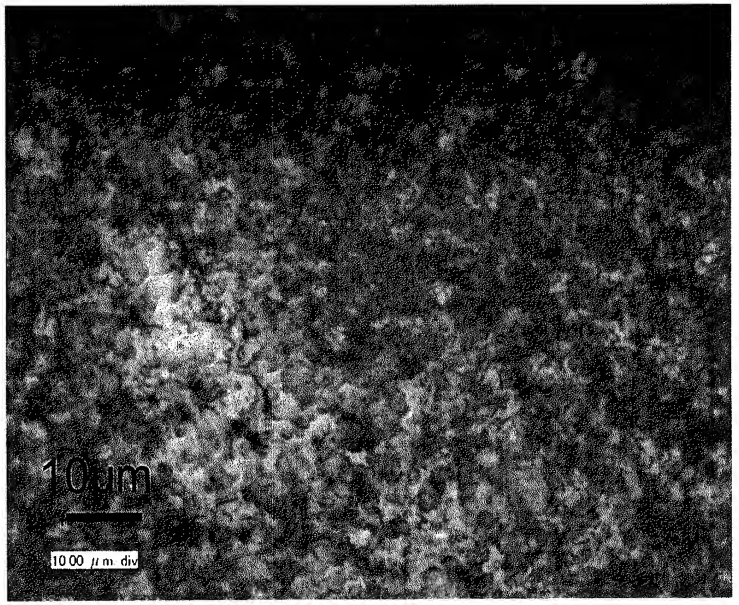

The surface is mottle as shown below. The structure varies by location and is not honeycomb one.

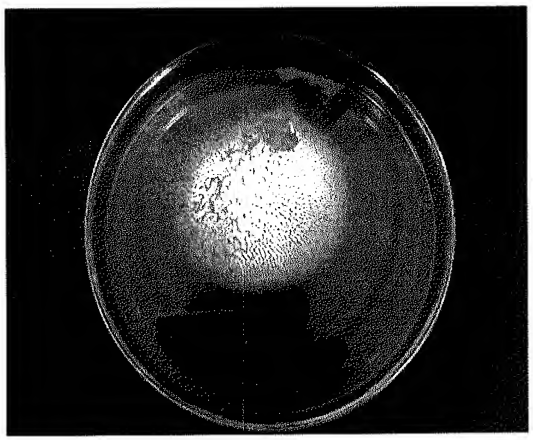

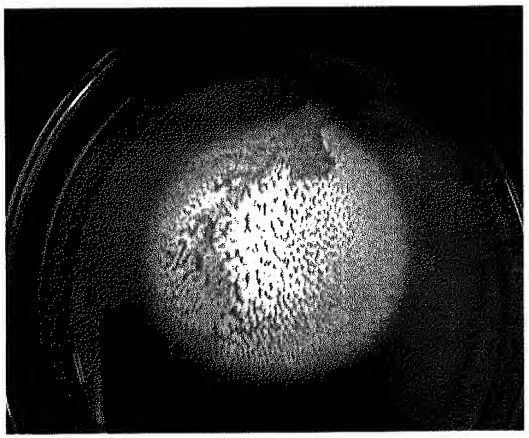

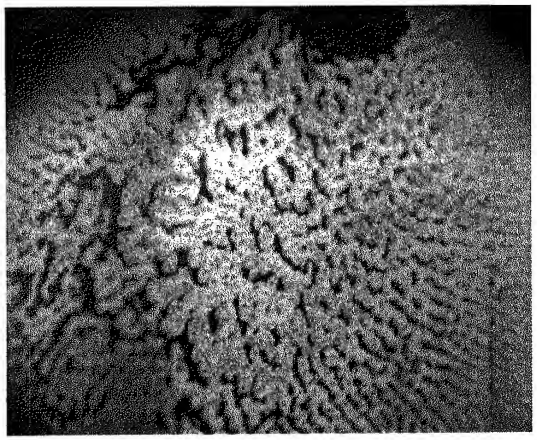

Entire picture: There is nonuniformity on the surface of the sheet.

Fig. 4

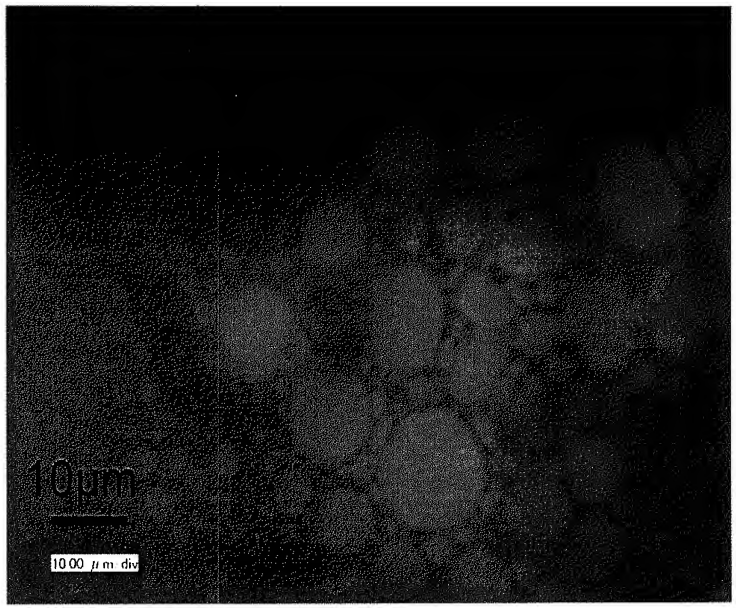

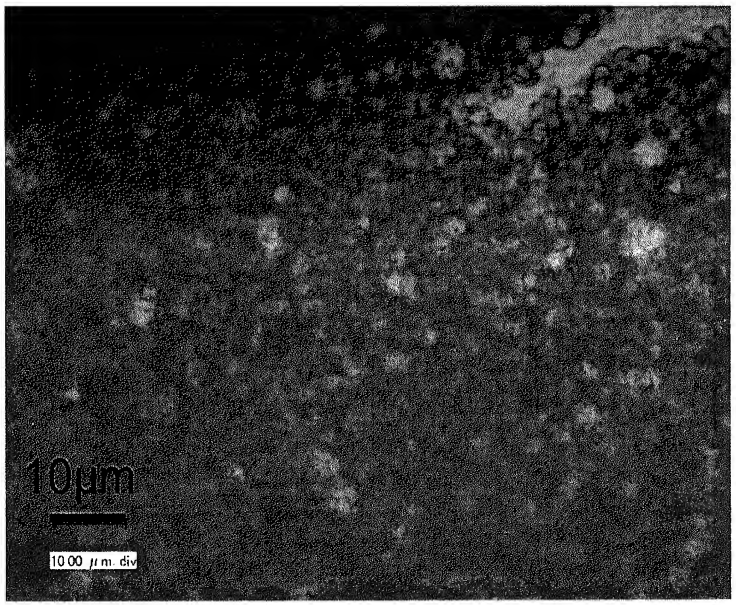

As a result of surface irregularity, these do not focus. These are not honeycomb structure in any event.

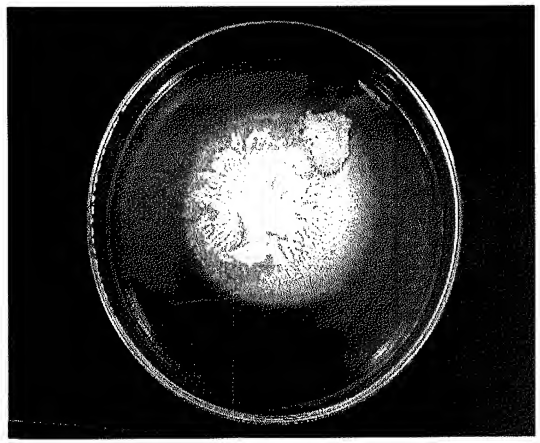

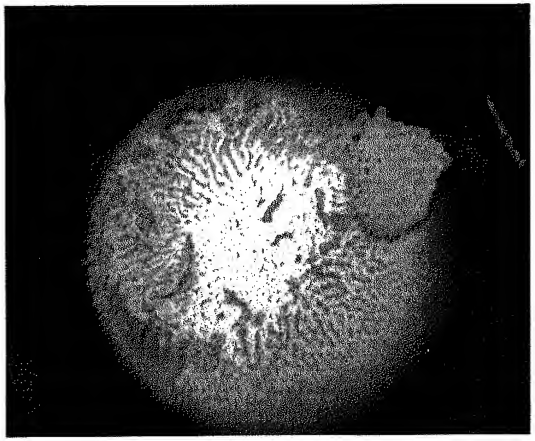

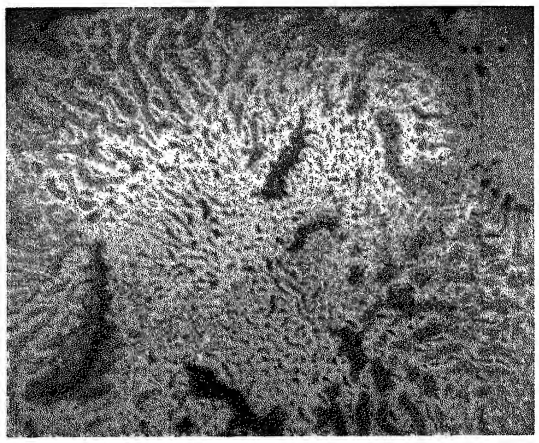

Entire picture: There is nonuniformity on the surface of the sheet.